# NFAT regulates the expression of AIF-1 and IRT-1: Yin and yang splice variants of neointima formation and atherosclerosis.

Berglund, Lisa; Kotova, Olga; Osmark, Peter; Grufman, Helena; Xing, Chen; Lydrup, Marie-Louise; Goncalves, Isabel; Autieri, Michael V; Gomez, Maria

*Published in:*
Cardiovascular Research

*DOI:*
10.1093/cvr/cvr309

2012

**NFAT regulates the expression of AIF-1 and IRT-1: yin and yang splice variants of neointima formation and atherosclerosis.** **Lisa M. Berglund, Olga Kotova, Peter Osmark, Helena Grufman, Chen Xing, Marie-Louise Lydrup, Isabel Goncalves, Michael V. Autieri & Maria F. Gomez.**

Aims: Alternative transcription and splicing of the Allograft Inflammatory Factor-1 (AIF-1) gene results in the expression of two different proteins: AIF-1 and Interferon Responsive Transcript-1 (IRT-1). Here we explore: 1) the impact of AIF-1 and IRT-1 on vascular smooth muscle cell (VSMC) activation and neointima formation, 2) mechanisms underlying their alternative splicing and 3) associations of AIF-1 and IRT-1 mRNA with parameters defining human atherosclerotic plaque phenotype.

Methods and results: Translation of AIF-1 and IRT-1 results in different products with contrasting cellular distribution and functions. Over expression of AIF-1 stimulates migration and proliferation of human VSMCs, whereas IRT-1 exerts opposite effects. Adenoviral infection of angioplasty injured rat carotid arteries with AdAIF-1 exacerbates intimal hyperplasia, whereas infection with AdIRT-1 reduces neointima. Expression of these variants is modulated by changes in Nuclear Factor of Activated T-cells (NFAT) activity. Pharmacological inhibition of NFAT or targeting of NFATc3 with siRNA lowers AIF-1/IRT-1 ratio and favors an anti-proliferative outcome. NFAT acts as a repressor on IRT-1 transcriptional start, a site also sensitive to interferon (IFN)γ stimulation. Expression of AIF-1 mRNA in human carotid plaques associates with less extracellular matrix and a more pro-inflammatory plaque and plasma profile, features that may predispose to plaque rupture. Instead, expression of IRT-1 mRNA associates with a less aggressive phenotype and less VSMCs at the most stenotic region of the plaque.

Conclusions: Inhibition of NFAT signaling, by shifting the AIF-1/IRT-1 ratio, may be an attractive target to regulate the VSMC response to injury and manipulate plaque stability in atherosclerosis.

CVR-2011-932R1

# NFAT regulates the expression of AIF-1 and IRT-1: Yin and yang splice variants of neointima formation and atherosclerosis

LISA M. BERGLUND[1], OLGA KOTOVA[1], PETER OSMARK[1], HELENA GRUFMAN[2], CHEN XING[3], MARIE-LOUISE LYDRUP[4], ISABEL GONCALVES[2], MICHAEL V. AUTIERI[3 §] & MARIA F. GOMEZ[1✉§]

*[1]Department of Clinical Sciences, Lund University, Malmö, Sweden; [2]Cardiology Department, Skåne University Hospital, Sweden; [3]Department of Physiology, Temple University School of Medicine, Philadelphia, PA, [4]Department of Surgery, Skåne University Hospital, Sweden.*

Running title: NFAT-dependent alternative splicing of AIF-1 and IRT-1

§ Authors contributed equally to this work

✉ Correspondence to:

Dept. of Clinical Sciences, Lund University,

CRC, entrance 72, building 91, level 12, 205 02 Malmö, Sweden.

E-mail: maria.gomez@med.lu.se.

Phone: +46-40-391058/Fax: +46-40-391212

Number of words in manuscript: 6145+250=6395

## INTRODUCTION

Vascular smooth muscle cell (VSMC) proliferation and migration after arterial injury results in occlusive neointima formation and plays a key role in the pathogenesis of restenosis after angioplasty, in-stent restenosis, allograft arteriopathy and vascular bypass graft occlusion.[1] Neointimal hyperplasia remains the major clinical limitation to vascular interventions and to long-term graft and recipient survival after organ transplantation.[2, 3] A common sequence of events, involving production of growth factors and cytokines by injured endothelium and inflammatory cells activates the normally quiescent VSMCs. Despite increased understanding of the pathogenesis of neointima formation, identification of novel molecular mechanisms that regulate VSMC migration and proliferation in response to injury and inflammation are necessary.

Allograft Inflammatory Factor-1 (AIF-1) and Interferon Responsive Transcript-1 (IRT-1) are alternatively transcribed and spliced mRNAs encoded from the AIF-1 gene within the MHC class III region of chromosome 6, a region densely populated with immune and inflammatory response genes (i.e. tumor necrosis factor α/β, NF-κB). AIF-1 was originally cloned from activated macrophages in cardiac allografts undergoing transplant rejection.[4] In the vasculature, AIF-1 protein increases after angioplasty and cytokine stimulation.[5] Expression levels are predictive of transplant vasculopathy and lowered after immunosuppressive therapy.[6] Over expression of AIF-1 increases VSMC migration and proliferation, whereas inhibition of AIF-1 exerts the opposite effect.[7, 8] Recent work using AIF-1 transgenic mice demonstrated that enhanced AIF-1 expression also increases atherosclerotic lesions.[9] Less is known regarding the role of the IRT-1 transcript, originally identified as an aberrant PCR product using AIF-1-specific primers and RNA from interferon-γ (IFNγ)-stimulated VSMCs.[10] Over expression of IRT-1 in human VSMCs seems to have anti-proliferative effects.[10]

The NFAT (Nuclear Factor of Activated T-cells) family of transcription factors consists of four members (NFATc1-c4), originally described as activators of cytokine and immunoregulatory genes in T-cells[11]. NFAT has been often implicated in the regulation of VSMC migration and proliferation[12] but the underlying mechanisms are far from clear. NFAT is readily activated by tyrosine kinase and G-protein coupled receptor stimulation, which is known to promote cell growth.[12] In a rat carotid artery injury model, blockade of NFAT signaling reduced neointima formation.[13] Recent work also shows that NFATc3 promotes VSMC proliferation and the expression of the pro-inflammatory and –atherogenic cytokines interleukin-6 (IL-6)[14] and osteopontin.[15]

In this study we describe differences in the genomic organization, in the 5' untranslated region (UTR) and in the cellular distribution of AIF-1 and IRT-1. We compare the impact of AIF-1 and IRT-1 over expression on neointima hyperplasia *in vivo* and provide evidence for the involvement of NFATc3 in the regulation of AIF-1 alternative splicing. Finally, we measure the expression levels of these transcripts in carotid plaques from patients undergoing endarterectomies to assess potential associations with plaque and clinical characteristics.

## MATERIALS & METHODS

Please see supplementary materials for an expanded version of this section.

*Human resistance arteries.* Intramyometrial arteries were used either directly after dissection or after organ culture.[14] This study conforms to the principles outlined in the Declaration of Helsinki and was approved by Lund University ethics review board (#LU39-02). All women gave their informed consent to participate.

*Cells.* Human myometrial vascular smooth muscle cells (VSMCs) were obtained from explants of myometrial arteries as previously described.[14] Human coronary artery smooth muscle cells (HCASMC) were from Cascade Biologics. Rat arterial VSMCs were prepared from explants of thoracic aorta as previously described.[16]

*Human carotid plaque biopsies.* 158 plaques collected at carotid endarterectomies and corresponding plasma samples were analyzed (Table 1). Indications for surgery were plaques associated with ipsilateral symptoms (transient ischemic attacks-TIA, stroke or amaurosis fugax) and stenosis >70%, or plaques not associated with symptoms but stenosis >80%. Plaques were snap-frozen and weighed; cross-sectional fragments from the most stenotic region were taken for histology, adjacent fragments for RNA isolation and the remaining plaque was homogenized as before[17] for protein and cytokine analyses. The study conforms to the principles outlined in the Declaration of Helsinki and was approved by Lund University ethics review board (#472/2005-LUND). All patients gave their informed consent to participate.

*In vitro transcription and translation.* Expression of AIF-1 and IRT-1 proteins was performed by coupled transcription (T3 polymerase) and translation using [$^{35}$S] Methionine in the TNT reticulocyte lysate system (Promega, Madison, WI). cDNA samples were cloned into pBlueScript vector

(Stratagene, La Jolla, CA). Reactions were analyzed on a 16.5% Tris-tricinepolyacrylamide gel (Biorad) and labeled proteins detected by autoradiography.

*Confocal microscopy.* Human VSMCs and myometrial artery sections were stained for AIF-1 and IRT-1 as previously described[14] and samples examined on a Zeiss LSM 5 laser scanning confocal microscope.

*Adenovirus construction.* Adenoviral HA-tagged AIF-1 and GFP have been previously described.[8] Recombinant adenovirus containing the IRT-1 gene was prepared using the AdEasy system in an identical way, with the IRT-1 coding region cloned into the shuttle vector pAdTrack-CMV.

*In vivo gene transfer and vessel morphometry.* Left common carotid artery balloon angioplasty was performed on male Sprague-Dawley rats as previously described,[8] under sodium-pentobarbital anesthesia [65 mg/kg, intraperitoneal (IP), Steris Laboratories, Phoenix, AZ]. Depth of anesthesia was assessed by the toe-pinch reflex procedure and absence of muscular tone. After injury, arteries were infected with adenoviral GFP, AIF-1 or IRT-1 or PBS for 15 minutes. Buprenorphine (0.02 mg/kg, subcutaneous) was given as analgesic pre- and 12 hours post-surgery. 14 days later, rats were exsanguinated via the vena cava under sodium-pentobarbital anesthesia (120 mg/kg, IP) and arteries harvested for morphometry. This study conforms to the *Guide for the Care and Use of Laboratory Animals* published by the US National Institutes of Health and was approved by the ethics board at Temple University (#3374).

*Proliferation and migration.* Rat VSMCs were infected with adenoviral GFP, AIF-1 or IRT-1 genes and proliferation and migration performed as previously described.[8]. Cells were infected at 30MOI for 2h for all experiments as we have described.[8] For human VSMCs, proliferation was measured using MTS-solution (CellTiter 96 $AQ_{ueous}$One Solution assay, Promega, Madison, WI).

*Western blot.* Protein was extracted from VSMCs and human myometrial arteries as previously described.[14] Primary antibodies against AIF-1, IRT-1, NFATc3 (sc-8321, Santa Cruz Biotechnology), GAPDH (Chemicon) and β-actin (GenScript Corporation, Piscataway, NJ); and HRP-conjugated secondary antibodies were used and proteins visualized by chemiluminescence.

*RNA isolation and RT-PCR.* RNA was isolated from myometrial arteries, VSMCs and carotid plaques followed by reverse transcription. cDNA was amplified using primers spanning regions common to both AIF-1 and IRT-1 splice variants and amplicons separated by agarose gel electrophoresis. For quantification, real-time PCR using TaqMan Gene Expression Assays (Applied Biosystems) and the comparative threshold method (delta Ct-method) were used.

*Small interfering RNA (siRNA) transfection.* Human VSMCs were transfected with NFATc3 ON-TARGET plus SMART pool siRNA or siCONTROL Non-Targeting siRNA pool (Dharmacon), complexed with Lipofectamine 2000 (Invitrogen) as previously described.[14]

*DNA Constructs, transfections and luciferase reporter assay.* A region of the human AIF-1 gene 5'-flanking region spanning from -1529 to +231 relative to AIF-1 translation start site was cloned into the pGL3 Basic Vector (Promega). Mutations were introduced using the QuikChange Site-Directed Mutagenesis Kit (Stratagene). HCASMC were transfected with plasmid DNA (wild-type or mutated AIF-1) or empty pGL3 basic vector (Promega Corporation, WI, USA) complexed with Lipofectamine 2000 (Invitrogen). Luminescence was measured as before.[14]

*Cytokines and plaque immunohistochemistry.* Cytokines were measured in aliquots of human carotid plaque homogenates or plasma (Milliplex Kit-Human Cytokine/Chemokine Immunoassay, Millipore, Electrabox Diagnostica AB, USA). Extracellular matrix components were determined

as before.[17] Human carotid plaque sections were stained for macrophages (CD68), smooth muscle cells (α-actin), lipids (Oil Red O) and collagen (Masson's trichrome).

*Statistics.* Results are expressed as means±SD. Statistical analysis was performed using GraphPad (Prism4.0) or SPSS version 17.0. Statistical significance was determined using two-tailed Student's t-test or Mann-Whitney non-parametric test, one-way analysis of variance followed by Bonferroni test and bivariate correlation analysis (*$p<0.05$, **$p<0.01$ and ***$p<0.001$).

## RESULTS

*AIF-1 and IRT-1 are differentially spliced products of the AIF-1 gene.* Several isoforms of the AIF-1 gene have been reported,[18] the two most characterized being AIF-1 and IRT-1. A graphic organization of the gene is represented in Supplemental Fig. S1. AIF-1 is composed of six exons and five introns spanning a genomic region of ~1800 nucleotides. The AIF-1 protein is translated from all six exons and results in a 143 amino acid protein of approximately 16.6 kDa. In contrast, IRT-1 is composed of only two exons and one intron. The entire IRT-1 protein is derived from exon two, which contains an open reading frame (ORF) of 399 nucleotides encoding a deduced 132 amino acid protein with a mass of approximately 14.5 kDa.

*IRT-1 mRNA contains an atypical 5' untranslated region (UTR).* To confirm translation of the ORF into the deduced gene products, AIF-1 and IRT-1 were expressed *in vitro*; either from cDNA containing only the ORF, or from full-length cDNA containing both the ORF and UTRs (Fig. 1A). For AIF-1, when the input sequence was from full-length 639 nt cDNA, expression levels were nearly identical to those obtained from the 429 nt ORF. In contrast, for IRT-1, using full-length cDNA yielded lower protein expression than when using the ORF alone. This suggests that at least *in vitro*, the 5' and/or 3' UTRs of IRT-1 decrease the efficiency of protein production. The secondary structure of the 74 nt long 5' UTRs for AIF-1 had a predicted change in free energy of -26.3 kcal/mol, while for IRT-1, the 453 nt long 5' UTR formed an extensive stem loop structure with a predicted change in free energy of -161.6 kcal/mol (Supplemental Fig. S2). The IRT-1 5' UTR further contained two short upstream ORFs (8 and 18 amino acids), which together with the longer more complex secondary structure may contribute to lower translation efficiency.[19] 90% of vertebrate mRNAs contain 5' UTRs that are 10-200 nt long, whereas mRNAs encoding growth factors, transcription factors or proto-oncogenes often have longer 5' UTRs.[19]

*Differential cellular localization of AIF-1 and IRT-1.* AIF-1 contains a functional EF-hand calcium binding domain required for inducing VSMC proliferation and migration.[5, 20] This domain is disrupted in the IRT-1 protein (Fig. 1B). Instead, IRT-1 contains a basic region immediately followed by a consensus leucine zipper motif, a four amino acid core nuclear localization sequence, and a single, strongly hydrophobic region,[10] all characteristics of transcription factors.[21] Using confocal immunofluorescence microscopy, we found that IRT-1 is predominantly nuclear, whereas AIF-1 is mainly cytosolic (Fig. 1C).

*Opposing effects of AIF-1 and IRT-1 on neointima formation after arterial injury in vivo.* Rat carotid arteries were injured by balloon angioplasty and then infected with recombinant adenovirus encoding AIF-1 (AdAIF-1), IRT-1 (AdIRT-1) or green fluorescent protein (AdGFP). PBS was used as vehicle control. A distinct neointima was observed 14 days later in injured control arteries not exposed to adenovirus (Fig. 2A). No neointima was formed in contralateral uninjured carotid arteries (data not shown). In arteries infected with AdAIF-1, neointima area was significantly larger when compared to AdGFP or control arteries (Fig. 2B). Arteries infected with AdIRT-1 instead, displayed reduced neointima area compared to AdGFP or vehicle (Fig. 2B). The effect of AdIRT-1 also resulted in reduced neointima/media ratio (Fig. 2C) and larger lumen area (Fig 2A and D).

To verify successful infections, AIF-1-HA, IRT-1 and GFP expression was examined (Supplemental Fig. S3). HA protein was detected in AdAIF-1 infected arteries, whereas no signal was observed in sections from injured control, AdGFP or AdIRT-1 infected arteries. HA tagged AIF-1 was used to specify exogenous expression, since endogenous AIF-1 is expressed in the media and constitutively expressed in leukocytes[8]. Despite non-specific binding of anti-GFP antibody to the adventitia of all vessels, only those that had been infected with AdGFP showed intense GFP expression in the neointima. IRT-1 protein was expressed only in vessels that had been infected with AdIRT-1.

*Differential effect of AIF-1 and IRT-1 over expression on VSMC proliferation and migration.* Primary VSMCs were infected with AdAIF-1 or AdIRT-1 and proliferation was compared to cells that had been infected with AdGFP. Over expression was confirmed by western blotting using antibodies against AIF-1 or IRT-1, respectively (Fig. 3A). Equal number of cells were seeded into 12-well plates 24h after transduction and cultured for 4 and 7 days in medium containing 10% FBS. Over expression of AIF-1 yielded increased cell number at day 7, while over expression of IRT-1 had the opposite effect (Fig. 3B). Infected VSMCs were also seeded into Boyden chambers and allowed to migrate towards a PDGF stimulus. Compared to AdGFP control cells, AIF-1 over expression resulted in a larger number of migrated cells whereas IRT-1 had the opposite effect (Fig. 3C).

*NFAT regulates AIF-1 and IRT-1 mRNA expression.* Analysis of the murine and human AIF-1 and IRT-1 promoters reveals theoretical binding sites for a wide range of transcription factors,[18] however, limited functional evidence is available. Sibinga et al[22] showed in murine macrophages that AIF-1 promoter activity was regulated by transcription factor binding to consensus Ets and interferon regulatory factor elements. In VSMCs, one transcription factor that has emerged as a regulator of cell proliferation and migration is NFAT.[12, 14] A search for NFAT consensus binding elements (5'-T/AGGAAA-3'[11]) in the 5' flanking region of AIF-1 and IRT-1 reveals the presence of four sites (Supplemental Fig. S4).

We next investigated whether changes in NFAT activity had any impact on the expression of AIF-1 and IRT-1, using primers that simultaneously detect both splice variants. Under basal conditions, AIF-1 mRNA is expressed in human VSMCs whereas no or little IRT-1 mRNA is detected (Fig. 4A). This is curious, since IRT-1 protein was detected in VSMCs under the same conditions (Fig. 1C). Incubation with Et-1, which is a potent stimulus for NFAT activation in these cells,[14] reduced the expression of AIF-1. This was prevented by the NFAT blocker A-285222. Et-1 stimulation had no apparent effect on IRT-1 levels; however, concomitant inhibition of NFAT increased expression of this transcript (Fig. 4A). The same was true when VSMCs were

cultured with A-285222 alone (Supplemental Fig. S4). In contrast to cultured cells, both AIF-1 and IRT-1 transcripts were detected in freshly isolated human arteries, at apparently equal levels (Fig. 4B). Upon organ culture of the arteries, which is associated with a well-characterized transition of the VSMCs towards a dedifferentiated phenotype,[23] expression of these splice variants shifted, with a relative increase of pro-proliferative AIF-1 compared to IRT-1. Coincidentally, NFAT activity is increased during culture of intact arteries, as well as the levels of IL-6.[14] Inhibition of NFAT signaling with A-285222 prevented this shift, increasing instead the relative abundance of the anti-proliferative variant IRT-1 (Fig.4B). This effect of NFAT inhibition was further confirmed by real-time RT-PCR (Fig. 4D) and was accompanied by increased IRT-1 protein as assessed by confocal immunofluorescence (Fig. 4C). Changes in IRT-1 protein were already evident after 3 days of culture with A-285222, as assessed by confocal immunofluorescence and western blot (Supplemental Fig.S5).

*NFAT inhibition leads to decreased proliferation and increased IRT-1 protein expression.* Pharmacological inhibition of NFAT with A-285222 for 48h reduced VSMC proliferation (Fig. 5A). Under the same conditions, IRT-1 protein was increased compared to control cells (Fig. 5B). To investigate the specific role of the NFATc3 isoform, siRNA against NFATc3 was used to down regulate its expression (Fig. 5C). IRT-1 protein expression was increased in cells expressing lower levels of NFATc3 (Fig. 5D).

*Mutation of NFAT binding site at the IRT-1 transcriptional start compromises IFNγ and A-285222-induced transcription.* One of the four NFAT consensus binding elements found in the AIF-1/IRT-1 promoter is located at the IRT-1 transcriptional start. To test its potential functional relevance, we used luciferase constructs driven by a ~2kb region of the AIF-1/IRT-1 promoter containing a mutation in this site (Supplemental Fig. S6). Incubation of VSMCs carrying the wild-type construct with A-285222 resulted in enhanced luciferase activity, whereas the response was

abrogated in cells transfected with the mutated construct (Fig. 6A). This NFAT binding site overlaps with a GAAANN motif, which is prevalent in IFN-induced genes.[24] Since IRT-1 is strongly upregulated by IFNγ,[10] the functional relevance of this site for IFNγ-induced transcription was tested. Stimulation of VSMCs carrying the wild-type construct with IFNγ resulted in enhanced luciferase activity, whereas no response was observed in cells carrying the mutated one. Hence, under non-stimulated conditions, NFAT appears to act on this site as a transcriptional repressor of IRT-1. Incubation with A-285222 would release the block, allowing IRT-1 transcription. This site may also be important for IFNγ-induced IRT-1 transcription, probably via displacement of NFAT from this site, as suggested by the lack of synergy between A-285222 and IFNγ. A cartoon summarizing the proposed mechanism is depicted in Fig. 6B.

*Differential associations of AIF-1 and IRT-1 expression with human plaque phenotype.* Human carotid plaques and plasma were collected from 158 patients undergoing endarterectomy to assess potential associations between plaque AIF-1 or IRT-1 mRNA expression with plaque and clinical characteristics. All patients had advanced atherosclerosis disease given that the indications for surgery were either ipsilateral symptoms (transient ischemic attacks-TIA, stroke or amaurosis fugax) and stenosis greater than 70%, or stenosis>80%. A brief clinical description of the patients is shown in Supplemental Table 1.

Inflammation is pivotal in the development of arterial lesions and high content of inflammatory cells and/or mediators are indicators of plaque vulnerability.[25] Here we found a positive association between AIF-1 mRNA and levels of plaque macrophage inflammatory protein (MIP)-1β and plasma RANTES. Instead, IRT-1 mRNA associated positively with plaque levels of the anti-inflammatory cytokine IL-10 and negatively with plasma monocyte chemoattractant protein (MCP)-1. Both transcripts exhibited positive associations to plaque IL-1β.

Analysis of extracellular matrix components in plaque homogenates revealed that AIF-1 levels were associated to lower collagen and elastin contents, whereas both transcripts showed

negative associations with levels of glycosaminoglycans. Examination of histological sections from the most stenotic region of the plaque showed that both transcripts were positively associated to the size of the lipid pool (Oil Red O) and degree of macrophage infiltration (CD68); and negatively associated to collagen (Masson). Interestingly, we found a negative association between IRT-1 mRNA and VSMC content (α-actin), maybe reflecting a decreased VSMC proliferation in patients with high IRT-1 levels. Sections also showed a positive association between AIF-1 mRNA and elastin, in contrast to that found in plaque homogenates from below and above the most stenotic region. Further, AIF-1 mRNA levels were positively associated with blood hemoglobin and age. A complete list of the parameters analyzed is shown in Supplemental Table 2.

## DISCUSSION

This study describes the alternative transcription and splicing of the AIF-1 gene, which results in the expression of two different proteins: AIF-1 and IRT-1. These proteins have opposite impact on angioplasty-induced neointima formation and on VSMC activation. We demonstrate that expression of these AIF-1 gene products is modulated by changes in NFAT activity. Moreover, we found differential associations of AIF-1 and IRT-1 mRNA levels with parameters defining human atherosclerotic plaque phenotype.

The major findings are: 1) IRT-1 mRNA contains an atypical 5' UTR which affects translational efficiency; 2) IRT-1 is primarily nuclear as opposed to a predominantly cytosolic AIF-1; 3) over expression of the anti-proliferative splice variant IRT-1 reduces neointima formation after angioplasty, whereas over expression of the pro-proliferative variant AIF-1 exerts the opposite effect; 4) consensus NFAT binding elements are present in the AIF-1/IRT-1 promoters; 5) changes in NFAT activity modulate AIF-1 and IRT-1 expression, with inhibition of NFAT resulting in lowered AIF-1/IRT-1 ratio and favoring an anti-proliferative outcome; 6) NFAT acts as a repressor on IRT-1 transcriptional start, a site also sensitive to IFNγ stimulation; and 7) expression of AIF-1 mRNA in human carotid plaques associates with less extracellular matrix contents and a more pro-inflammatory plaque and plasma profile, features that may predispose to plaque rupture. Instead, expression of IRT-1 mRNA associates with a less aggressive phenotype and less VSMCs at the most stenotic region of the plaque. Thus, AIF-1 and IRT-1 seem to behave as yin and yang variants with opposite impact on neointima formation and atherosclerosis.

Clear differences were observed in the length and predicted secondary structure of the 5' UTRs of AIF-1 and IRT-1. The long and highly structured IRT-1 5' UTR and the presence of two upstream ORFs are sequence characteristics which can decrease translational efficiency and are shared by growth regulatory genes.[19] A third attribute of IRT-1 is the long 3' UTR containing an ATTTA sequence, typically found in the mRNA of cytokines and proto-oncogenes and thought to

confer mRNA instability.[10] The presence of AU-rich elements that can increase mRNA turnover via deadenylation and degradation, may explain the discrepancy between IRT-1 mRNA and protein levels observed (Fig. 4A vs. Fig 1C). IRT-1 mRNA is indeed unstable, with 50% degradation after 8.5h and 75% degradation after 16h.[26] The described regulatory elements are consistent with a role for IRT-1 in the regulation of cell proliferation.

Fundamental differences are also found between AIF-1 and IRT-1 at the protein level. The structure of AIF-1 is of a cytoplasmic, calcium-binding signal transduction/scaffold protein.[20] IRT-1 instead, has sequence signatures of a nuclear, DNA-binding protein. At the present time, the structure/function relationships for AIF-1 and IRT-1 are uncharacterized, and beyond the scope of the present study. However, these protein characteristics may explain the differences in their intracellular distribution.

Over expression of AIF-1 and IRT-1 regulates VSMC proliferation and migration and this is likely one mechanism underlying the *in vivo* changes in neointima formation after balloon injury. We cannot rule out that other cell types in the vessel wall apart from VSMCs are infected during the incubation with the different adenoviruses, but the endothelium was almost completely removed after angioplasty and no inflammatory cells were observed at the time of infection, making this alternative explanation less likely. Furthermore, when ligation injury of the carotid artery was performed in transgenic mice in which AIF-1 expression is restricted to VSMCs (driven by a modified SM22α promoter), an enhanced response to injury was still obtained.[7]

NFAT activity has a pronounced inhibitory effect on IRT-1, which would suggest that NFAT acts as a repressor. Three of the NFAT-binding elements (NFAT sites 2-4) are located in a region that was described to have predominantly repressive effects on promoter activity.[22] Abundant evidence support the role of NFAT as a transcriptional activator, but a regulatory role for NFAT as suppressor is also emerging. An interesting example is NFATc2, which was shown in

immune cells to suppress cyclin-dependent kinase 4 expression through binding to a site immediately downstream of the transcriptional start site.[27] The promoter studies described here support the idea of NFAT acting as a repressor of IRT-1 at NFAT site 1, located immediately downstream of the IRT-1 transcriptional start site. This site may also be relevant for IFNγ-induced transcription of IRT-1. IFNγ has anti-proliferative actions on VSMC[28, 29] and inhibits angioplasty-induced arterial restenosis.[28, 30] It is possible that part of the anti-proliferative program of IFNγ may involve regulation of AIF-1 alternative splicing to favor IRT-1 expression, and that this utilizes the NFAT site 1 described here.

The opposite roles of AIF-1 and IRT-1 may not be just limited to the context of neointima formation. Their differential associations with atherosclerotic plaque phenotype and plasma parameters in patients undergoing endarterectomies suggest they may also exert different roles in human atherosclerosis. Higher AIF-1 expression associated with a more pro-inflammatory profile than IRT-1, which instead associated positively with anti-inflammatory IL-10 in the plaque. Endogenous production of IL-10 in the vessel wall limits angiotensin II-mediated oxidative stress and vascular dysfunction and may account for the protective effects exerted by this cytokine.[31]

Collagen contents increase in parallel with the evolution of the lesions, but in advanced plaques as the ones examined here, extensive degradation of collagen occurs in the lipid and necrotic core, contributing to weakening and fragility.[32] AIF-1 but not IRT-1 levels associated negatively with plaque collagen. A similar pattern was observed for elastin measured from plaque homogenates (i.e. patients with high expression of AIF-1 had lower elastin contents). Higher elastin breakdown results in loss of medial elasticity, increased luminal wall stress and subsequently, increased endothelial damage and predisposition to atherosclerosis.[33] This is in line with recent work showing that AIF-1 transgenic mice had increased atherosclerosis and higher expression of the matrix metalloproteinases MMP2 and MMP9 in VSMCs,[34] both strongly correlated with

plaque instability.[35] On the other hand, AIF-1 associated positively to histologically determined elastin contents from sections at the most stenotic region of the plaque. This is the area where VSMCs are most abundant and these cells are the main producers of elastin in the plaque.[32] Results are intriguing, but at the moment we cannot provide an explanation for the opposite relationships between AIF-1 and elastin at different sites of the plaque.

Additionally, a positive association between AIF-1 and blood hemoglobin was found. Just recently, the Apolipoprotein MOrtality RISk (AMORIS) Study including over 114.000 patients established high blood hemoglobin as risk factor for major atherosclerotic cardiovascular events, including acute myocardial infarction, congestive heart failure and stroke.[36] Hemoglobin seems to contribute to plaque instability by triggering chemotaxis of monocytes and dendritic cells into the vascular wall.[37] In summary, plaque expression of AIF-1 associates with more inflammatory and rupture prone plaque phenotype, whereas IRT-1 associates with more beneficial parameters. Inhibition of the NFAT signaling pathway, by shifting the AIF-1/IRT-1 ratio, may be an attractive target to regulate the VSMC response to injury and manipulate plaque stability in atherosclerosis.

***FUNDING***

This work was supported by the Swedish Heart and Lung Foundation [HLF20070459 and HLF20080843 to M.F.G., HLF20090419 to I.G.]; the Swedish Research Council [2006-5287 and 2009-4120 to M.F.G.; 2010-2932 to I.G.]; the National Heart Lung, and Blood Institute [HL-63810 to M.V.A.]; the American Heart Association [0455562U to M.V.A.] and the Roche Organ Transplant Research Foundation [146643428 to M.V.A.]. Also by the Swedish Medical Society; Crafoord; Påhlsson; Hierta Memorial; Wiberg; Zoéga; Lundström; Lundgren; Nilsson; Segerfalk; M&M Wallenberg; K&A Wallenberg foundations; Royal Physiographic Society in Lund; Skåne Hospital Research Funds; Regional Research Funds; Swedish Society for Medical Research, Vascular Wall Programme at the Medical Faculty in Lund and Lund University Diabetes Centre.

**ACKNOWLEDGEMENTS**

We thank Catarina Larsson, Mihaela Nitulescu, Ana Persson and Marie Nilsson for technical assistance. A-285222 was kindly provided by Abbott Laboratories (Abbott Park, IL).

**CONFLICT OF INTEREST**

None declared.

## REFERENCES

1. Crook MF, Akyurek LM. Gene transfer strategies to inhibit neointima formation. *Trends Cardiovasc Med* 2003;**13**:102-106.

2. Shimizu K, Mitchell RN. The role of chemokines in transplant graft arterial disease. *Arterioscler Thromb Vasc Biol* 2008;**28**:1937-1949.

3. Zargham R. Preventing restenosis after angioplasty: A multistage approach. *Clin Sci (Lond)* 2008;**114**:257-264.

4. Utans U, Arceci RJ, Yamashita Y, Russell ME. Cloning and characterization of allograft inflammatory factor-1: A novel macrophage factor identified in rat cardiac allografts with chronic rejection. *J Clin Invest* 1995;**95**:2954-2962.

5. Autieri MV. Cdna cloning of human allograft inflammatory factor-1: Tissue distribution, cytokine induction, and mrna expression in injured rat carotid arteries. *Biochem Biophys Res Commun* 1996;**228**:29-37.

6. Autieri MV, Kelemen S, Thomas BA, Feller ED, Goldman BI, Eisen HJ. Allograft inflammatory factor-1 expression correlates with cardiac rejection and development of cardiac allograft vasculopathy. *Circulation* 2002;**106**:2218-2223.

7. Sommerville LJ, Kelemen SE, Autieri MV. Increased smooth muscle cell activation and neointima formation in response to injury in aif-1 transgenic mice. *Arterioscler Thromb Vasc Biol* 2008;**28**:47-53.

8. Sommerville LJ, Xing C, Kelemen SE, Eguchi S, Autieri MV. Inhibition of allograft inflammatory factor-1 expression reduces development of neointimal hyperplasia and p38 kinase activity. *Cardiovasc Res* 2009;**81**:206-215.

9. Mishima T, Iwabuchi K, Fujii S, Tanaka SY, Ogura H, Watano-Miyata K *et al.* Allograft inflammatory factor-1 augments macrophage phagocytotic activity and accelerates the progression of atherosclerosis in apoe-/- mice. *Int J Mol Med* 2008;**21**:181-187.

10. Autieri MV, Agrawal N. Irt-1, a novel interferon-gamma-responsive transcript encoding a growth-suppressing basic leucine zipper protein. *J Biol Chem* 1998;**273**:14731-14737.

11. Rao A, Luo C, Hogan PG. Transcription factors of the nfat family: Regulation and function. *Annu Rev Immunol* 1997;**15**:707-747.

12. Liu Z, Dronadula N, Rao GN. A novel role for nuclear factor of activated t cells in receptor tyrosine kinase and g protein-coupled receptor agonist-induced vascular smooth muscle cell motility. *J Biol Chem* 2004;**279**:41218-41226.

13. Liu Z, Zhang C, Dronadula N, Li Q, Rao GN. Blockade of nuclear factor of activated t cells activation signaling suppresses balloon injury-induced neointima formation in a rat carotid artery model. *J Biol Chem* 2005;**280**:14700-14708.

14. Nilsson LM, Sun Z-W, Nilsson J, Nordstrom I, Chen Y-W, Molkentin JD *et al.* Novel blocker of nfat activation inhibits il-6 production in human myometrial arteries and reduces vascular smooth muscle cell proliferation. *Am J Physiol Cell Physiol* 2007;**292**:C1167-1178.

15. Nilsson-Berglund LM, Zetterqvist AV, Nilsson-Ohman J, Sigvardsson M, Gonzalez Bosc LV, Smith ML *et al.* Nuclear factor of activated t cells regulates osteopontin expression in arterial smooth muscle in response to diabetes-induced hyperglycemia. *Arterioscler Thromb Vasc Biol* 2010;**30**:218-224.

16. Autieri MV, Carbone CM. Overexpression of allograft inflammatory factor-1 promotes proliferation of vascular smooth muscle cells by cell cycle deregulation. *Arterioscler Thromb Vasc Biol* 2001;**21**:1421-1426.

17. Goncalves I, Moses J, Dias N, Pedro LM, Fernandes e Fernandes J, Nilsson J *et al.* Changes related to age and cerebrovascular symptoms in the extracellular matrix of human carotid plaques. *Stroke* 2003;**34**:616-622.

18. Deininger MH, Meyermann R, Schluesener HJ. The allograft inflammatory factor-1 family of proteins. *FEBS Lett* 2002;**514**:115-121.

19. Willis AE. Translational control of growth factor and proto-oncogene expression. *Int J Biochem Cell Biol* 1999;**31**:73-86.

20. Autieri MV, Chen X. The ability of aif-1 to activate human vascular smooth muscle cells is lost by mutations in the ef-hand calcium-binding region. *Exp Cell Res* 2005;**307**:204-211.

21. Amoutzias GD, Robertson DL, Van de Peer Y, Oliver SG. Choose your partners: Dimerization in eukaryotic transcription factors. *Trends Biochem Sci* 2008;**33**:220-229.

22. Sibinga NES, Feinberg MW, Yang H, Werner F, Jain MK. Macrophage-restricted and interferon gamma -inducible expression of the allograft inflammatory factor-1 gene requires pu.1. *J. Biol. Chem.* 2002;**277**:16202-16210.

23. Hellstrand P. Long-term effects of intracellular calcium and growth factors on excitation and contraction in smooth muscle. *Acta Physiol Scand* 1998;**164**:637-644.

24. Sims SH, Cha Y, Romine MF, Gao PQ, Gottlieb K, Deisseroth AB. A novel interferon-inducible domain: Structural and functional analysis of the human interferon regulatory factor 1 gene promoter. *Mol Cell Biol* 1993;**13**:690-702.

25. Libby P, Aikawa M. Stabilization of atherosclerotic plaques: New mechanisms and clinical targets. *Nat Med* 2002;**8**:1257-1262.

26. Del Galdo F, Maul GG, Jimenez SA, Artlett CM. Expression of allograft inflammatory factor 1 in tissues from patients with systemic sclerosis and in vitro differential expression of its isoforms in response to transforming growth factor beta. *Arthritis Rheum* 2006;**54**:2616-2625.

27. Baksh S, Widlund HR, Frazer-Abel AA, Du J, Fosmire S, Fisher DE *et al.* Nfatc2-mediated repression of cyclin-dependent kinase 4 expression. *Mol Cell* 2002;**10**:1071-1081.

28. Hansson GK, Jonasson L, Holm J, Clowes MM, Clowes AW. Gamma-interferon regulates vascular smooth muscle proliferation and ia antigen expression in vivo and in vitro. *Circ Res* 1988;**63**:712-719.

29. Rolfe BE, Campbell JH, Smith NJ, Cheong MW, Campbell GR. T lymphocytes affect smooth muscle cell phenotype and proliferation. *Arterioscler Thromb Vasc Biol* 1995;**15**:1204-1210.

30. Hansson GK, Holm J. Interferon-gamma inhibits arterial stenosis after injury. *Circulation* 1991;**84**:1266-1272.

31. Didion SP, Kinzenbaw DA, Schrader LI, Chu Y, Faraci FM. Endogenous interleukin-10 inhibits angiotensin ii-induced vascular dysfunction. *Hypertension* 2009;**54**:619-624.

32. Katsuda S, Kaji T. Atherosclerosis and extracellular matrix. *J Atheroscler Thromb* 2003;**10**:267-274.

33. Krettek A, Sukhova GK, Libby P. Elastogenesis in human arterial disease: A role for macrophages in disordered elastin synthesis. *Arterioscler Thromb Vasc Biol* 2003;**23**:582-587.

34. Sommerville LJ, Kelemen SE, Ellison SP, England RN, Autieri MV. Increased atherosclerosis and vascular smooth muscle cell activation in aif-1 transgenic mice fed a high-fat diet. *Atherosclerosis* **In Press, Accepted Manuscript**:

35. Heo SH, Cho C-H, Kim HO, Jo YH, Yoon K-S, Lee JH *et al.* Plaque rupture is a determinant of vascular events in carotid artery atherosclerotic disease: Involvement of matrix metalloproteinases 2 and 9. *J Clin Neurol* **7**:69-76.

36. Holme I, Aastveit AH, Hammar N, Jungner I, Walldius G. High blood hemoglobin concentration as risk factor of major atherosclerotic cardiovascular events in 114,159 healthy men and women in the apolipoprotein mortality risk study (amoris). *Ann Med* 2011;

37. Buttari B, Profumo E, Di Cristofano C, Pietraforte D, Lionetti V, Capoano R *et al.* Haemoglobin triggers chemotaxis of human monocyte-derived dendritic cells: Possible role in atherosclerotic lesion instability. *Atherosclerosis* **215**:316-322.

## FIGURE LEGENDS

**Figure 1. The IRT-1 protein contains a nuclear localization signal. A.** Coupled *in vitro* transcription and translation showing gene products expressed from 1 μg of AIF-1 full length cDNA (lane 1) or ORF (lane 2) and IRT-1 full length cDNA (lane 3) or ORF (lane 4). **B.** Protein sequences for AIF-1 (upper line) and IRT-1 (lower line): Calcium-binding EF-hand (underlined); core nuclear localization sequence (red) and leucine residues (blue) are shown. **C.** Confocal immunofluorescence images of human VSMCs stained for AIF-1 (upper left panel, red), IRT-1 (lower left panel, red) and SYTOX Green (middle panels, green). Right panels show merged images and yellow indicates co-localization of IRT-1 with nuclear staining. Bars: 50 μm.

**Figure 2. AIF-1 exacerbates restenosis after angioplasty in rat carotid artery, whereas IRT-1 reduces it. A.** The effect of adenoviral delivery of AIF-1, IRT-1 or GFP to balloon angioplasty-injured rat carotid arteries *in vivo* evaluated 14 days after injury in sections stained with hematoxylin-eosin. Scale bars=150 μm and 50 μm, for upper and lower panels respectively. Summarized data from morphometric analysis for **B.** neointimal, **C.** neointimal/media ratio and **D.** lumen area. *$p<0.05$ and ***$p<0.001$ vs. AdGFP, n=6 rats/group.

**Figure 3. Opposite effects of AIF-1 and IRT-1 on VSMC proliferation and migration. A.** Western blots confirming over expression of AIF-1 (upper panel) or IRT-1 (lower panel) in infected rat VSMCs. GAPDH was used to verify equal loading. **B.** Effect of AdAIF-1 and AdIRT-1 over expression on VSMC proliferation. Means from 3 independent experiments performed in triplicate. **C.** Migration of VSMCs infected with AdAIF-1, AdIRT-1 or AdGFP in response to PDGF-AB (40ng) for 3h. Mean number of migrated cells per high power field (HPF) from 3 independently infected groups performed in triplicate. *$p<0.05$ and **$p<0.01$ vs. AdGFP.

**Figure 4. NFAT inhibition increases AIF-1 and IRT-1 expression. A.** Agarose gels showing expression of AIF-1, IRT-1 and HPRT in human VSMCs, incubated with or without Et-1 (10 nM) for 30min in the presence or absence of A-285222 (1.0 μM). After stimulation, cells were further incubated in fresh medium for 18h before RNA extraction. Samples were run in triplicates and experiments repeated twice using cells from different patients. **B.** AIF-1 and IRT-1 mRNA expression in intact human myometrial arteries cultured for up to four days with or without A-285222 (1.0 μM). Primers detecting both AIF-1 and IRT-1 were used and graph shows the ratio between AIF-1 and IRT-1. **C.** Representative confocal images showing IRT-1 or AIF-1 protein expression (red) in sections from myometrial arteries that had been cultured for 4 days with or without A-285222 (0.1 μM). For each condition, sections from the same artery are shown in the upper and lower panels. Nuclei were stained with Sytox Green. Scale bars = 50 μm (n=4). **D.** Summarized data from quantitative real-time PCR showing AIF-1 and IRT-1 mRNA expression in human myometrial arteries cultured for 4 days as in B, normalized to HPRT and cyclophilin A and expressed as percentage of untreated control arteries. *$p<0.05$ and ***$p<0.001$ vs. control, n=4-7/group.

**Figure 5. NFATc3 inhibits IRT-1 expression. A.** Human VSMCs were incubated for 2 days in 15% FBS, with or without A-285222 (1.0 μM). Proliferation was measured by MTS assay and normalized to control (n=4). **B.** Representative western blot and summarized data from experiments showing IRT-1 protein levels in human VSMCs treated as in A. Data was normalized to GAPDH and expressed as percentage of control (n=4). **C/D.** Summarized data from western blot experiments showing NFATc3 (C) and IRT-1 (D) expression in human VSMCs 5 days after transfection with siNFATc3 (100 nM). Representative blots from the same gel show simultaneous downregulation of NFATc3 and upregulation of IRT-1 expression. Data was normalized to β-actin and expressed as percentage of control (siCONTROL, n=5).

**Figure 6. Inhibition of NFAT increases promoter activity. A.** HCASMC were transfected with plasmid DNA containing either the wildtype (WT) or mutated (mut) AIF-1/IRT-1 promoter, or empty pGL3 basic vector. After 24h, transfected cells were stimulated with 0.5-1 μg/mL (10-20000 units/mL) IFNγ, 1 μM A-285222 or IFNγ and A-285222 together. Non-stimulated transfected cells served as control. After 6h, cells were harvested and luciferase activity normalized to total protein content measured. Results are expressed relative to the untreated WT plasmid. The experiment was performed four times, each in triplicates. **B.** Proposed mechanism underlying NFAT- and IFNγ-dependent regulation of the AIF-1/IRT-1 promoter.

**A**

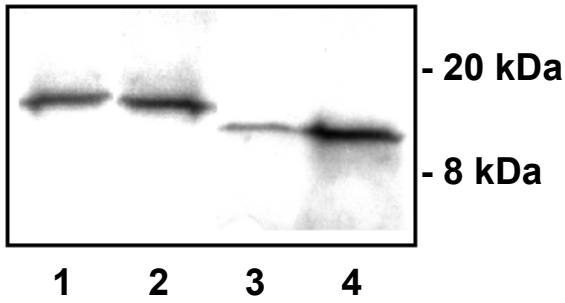


**B**

```
AIF-1       1   MSQTRDLQGG KAFGLLKAQQ EERLDEINKQ FLDDPKYSSD EDLPSKLEGF
IRT-1       1   ---------- ---------- ---------- ---------- ----------

AIF-1      51   KEKYMEFDLN GNGDI----- ---------- ---------- ----------
IRT-1       1   ----MEFDLN GNGDIGEKRV ICGGRVVCRP KKTEVSPTCS IPHDLGGGPP

AIF-1      66   ---------- ---------- ---------- -DIMSLKRML EKLGVPKTHL
IRT-1      47   TTVGGRRMGM RKWERRERVS PPSPHPHPLP PDIMSLKRML EKLGVPKTHL

AIF-1      85   ELKKLIGEVS SGSGETFSYP DFLRMMLGKR SAILKMILMY EEKAREKEKP
IRT-1      97   ELKKLIGEVS SGSGETFSYP DFLRMMLGKR SAILKM---- ----------

AIF-1     135   TGPPAKKAIS ELP
IRT-1     133   ---------- ---
```

**C**

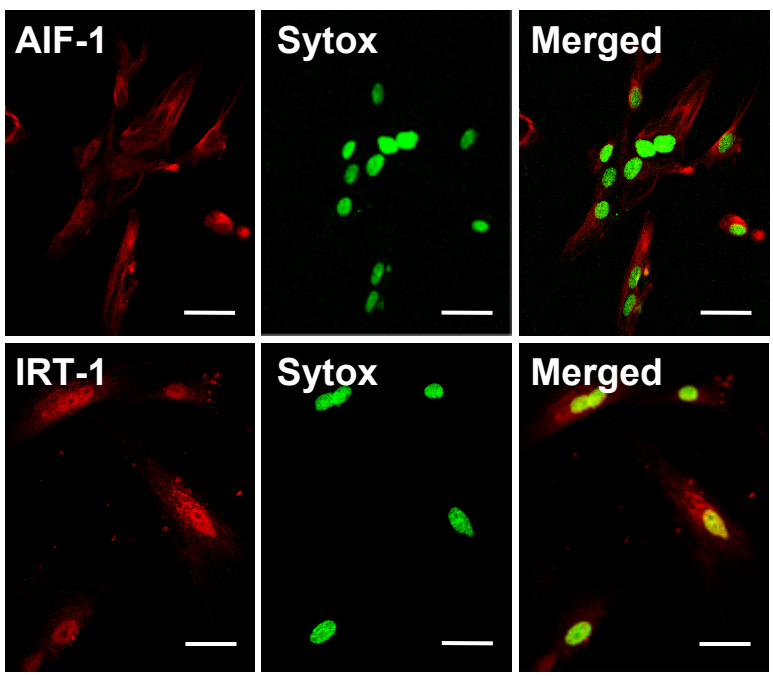


**Fig. 1**

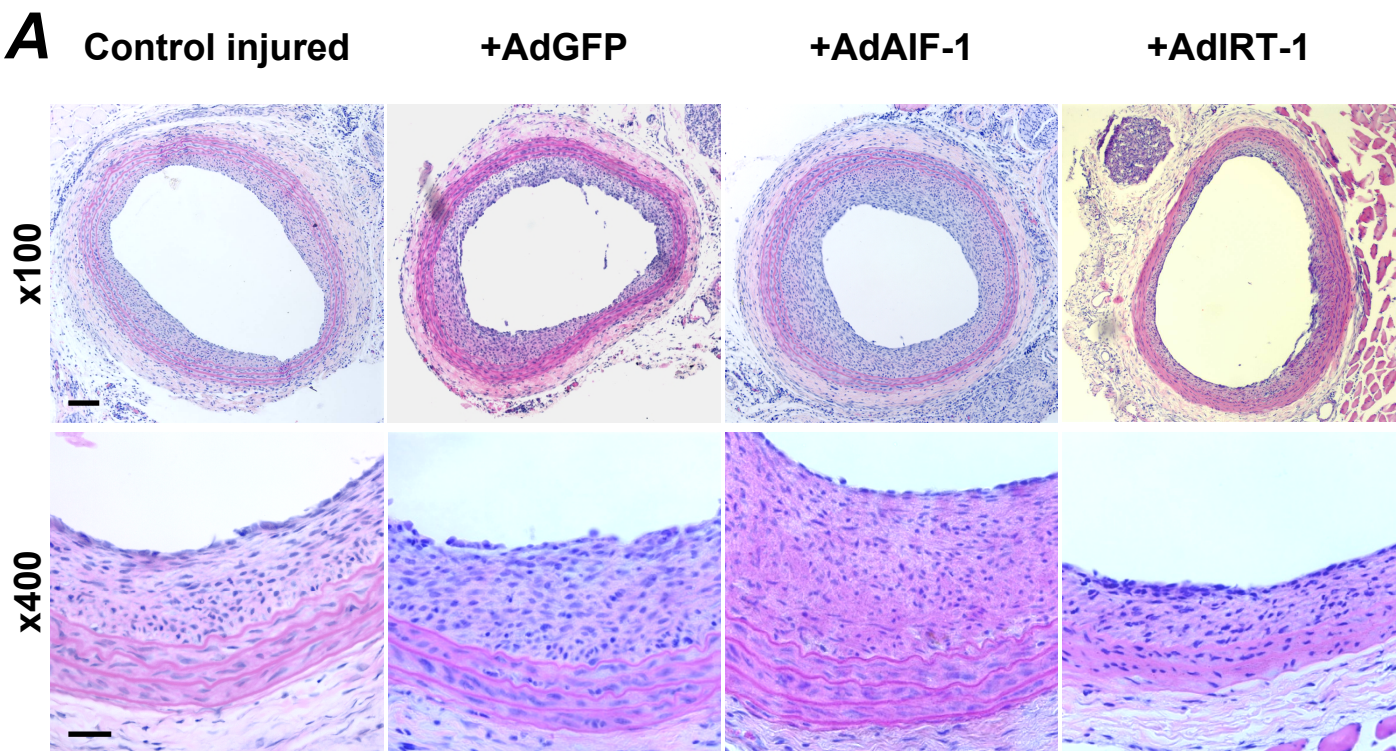
A
Control injured
+AdGFP
+AdAIF-1
+AdIRT-1
x100
x400

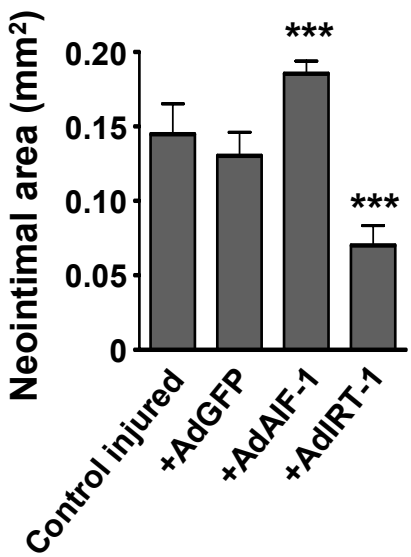
B
Neointimal area (mm²)
0.20
0.15
0.10
0.05
0
***
***
Control injured
+AdGFP
+AdAIF-1
+AdIRT-1

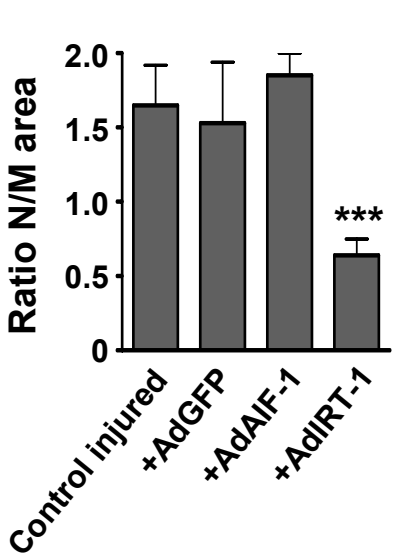
C
Ratio N/M area
2.0
1.5
1.0
0.5
0
***
Control injured
+AdGFP
+AdAIF-1
+AdIRT-1

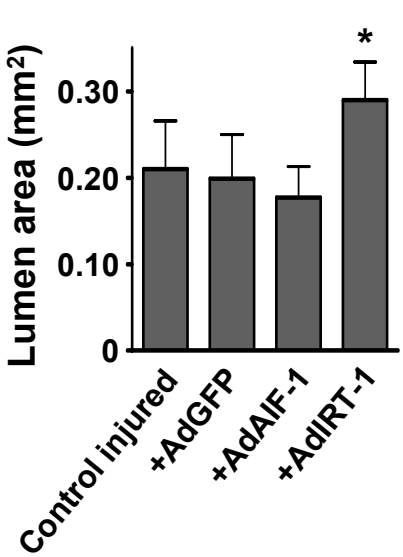
D
Lumen area (mm²)
0.30
0.20
0.10
0
*
Control injured
+AdGFP
+AdAIF-1
+AdIRT-1

Fig. 2

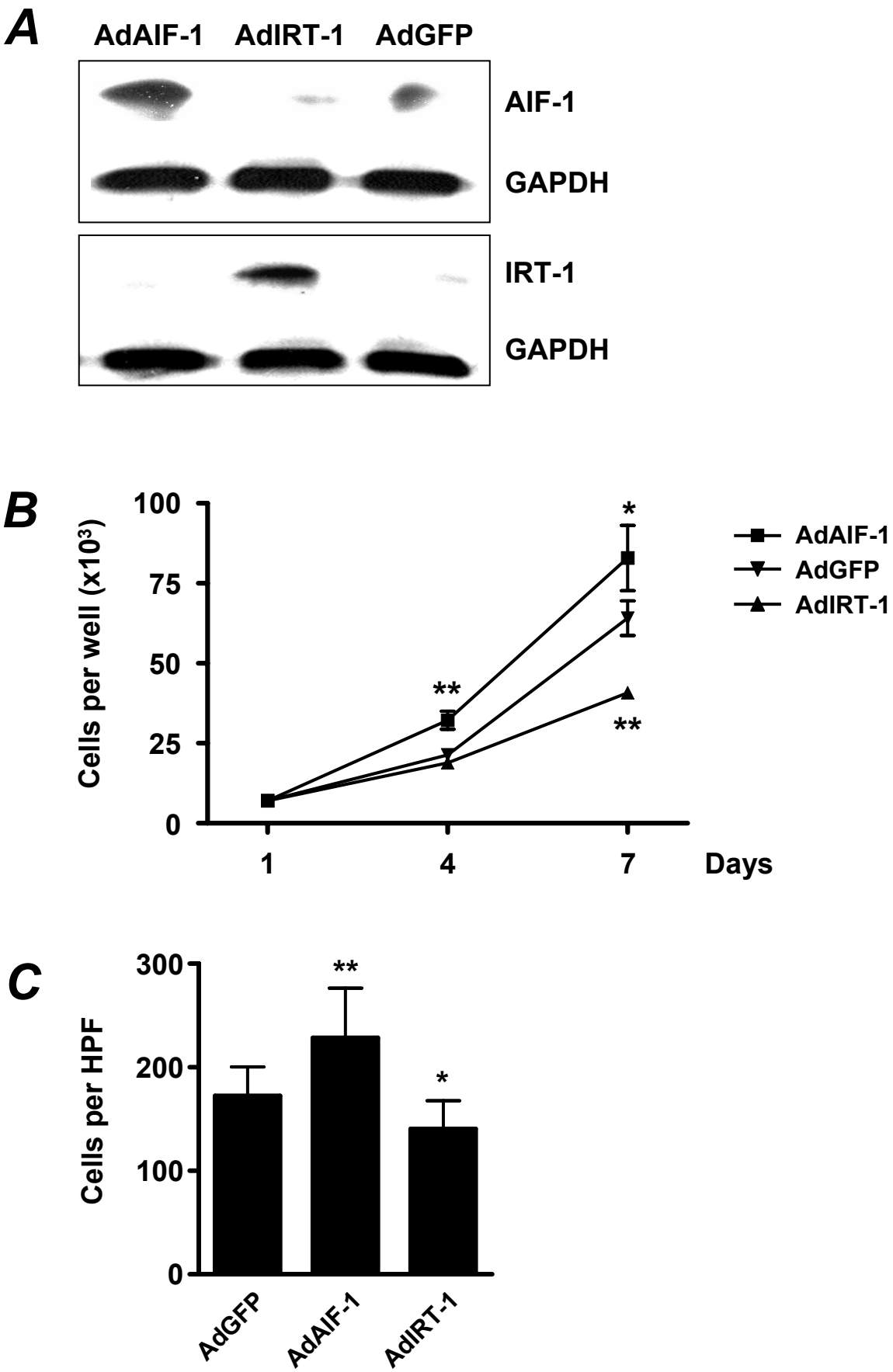
A
AdAIF-1
AdIRT-1
AdGFP
AIF-1
GAPDH
IRT-1
GAPDH
B
Cells per well (x10³)
100
75
50
25
0
1
4
7
Days
*
**
**
AdAIF-1
AdGFP
AdIRT-1
C
Cells per HPF
300
200
100
0
**
*
AdGFP
AdAIF-1
AdIRT-1

Fig. 3

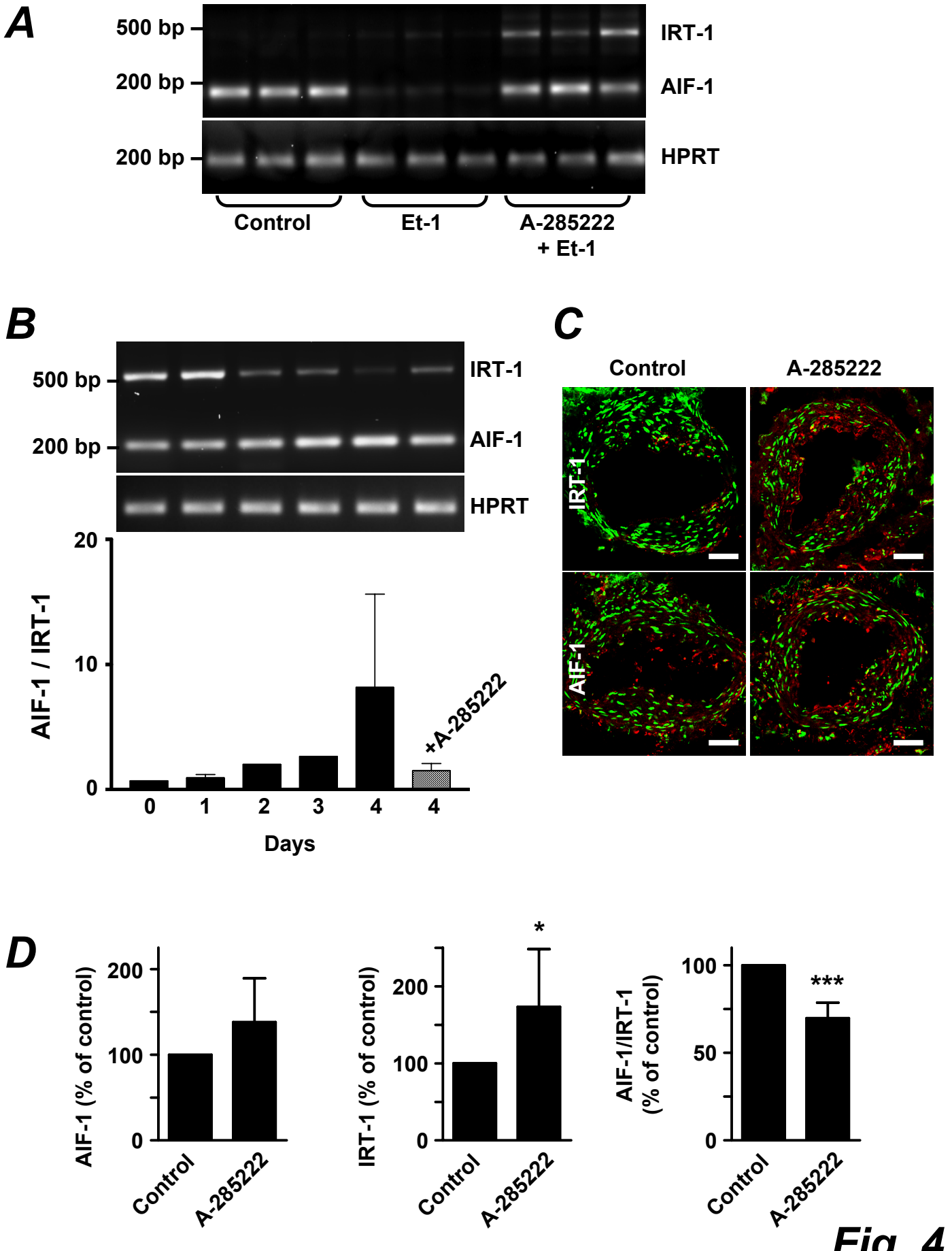
A
500 bp
200 bp
IRT-1
AIF-1
200 bp
HPRT
Control
Et-1
A-285222
+ Et-1
B
500 bp
200 bp
IRT-1
AIF-1
HPRT
AIF-1 / IRT-1
20
10
0
+A-285222
0
1
2
3
4
4
Days
C
Control
A-285222
IRT-1
AIF-1
D
AIF-1 (% of control)
200
100
0
Control
A-285222
IRT-1 (% of control)
*
200
100
0
Control
A-285222
AIF-1/IRT-1
(% of control)
100
50
0
***
Control
A-285222

Fig. 4

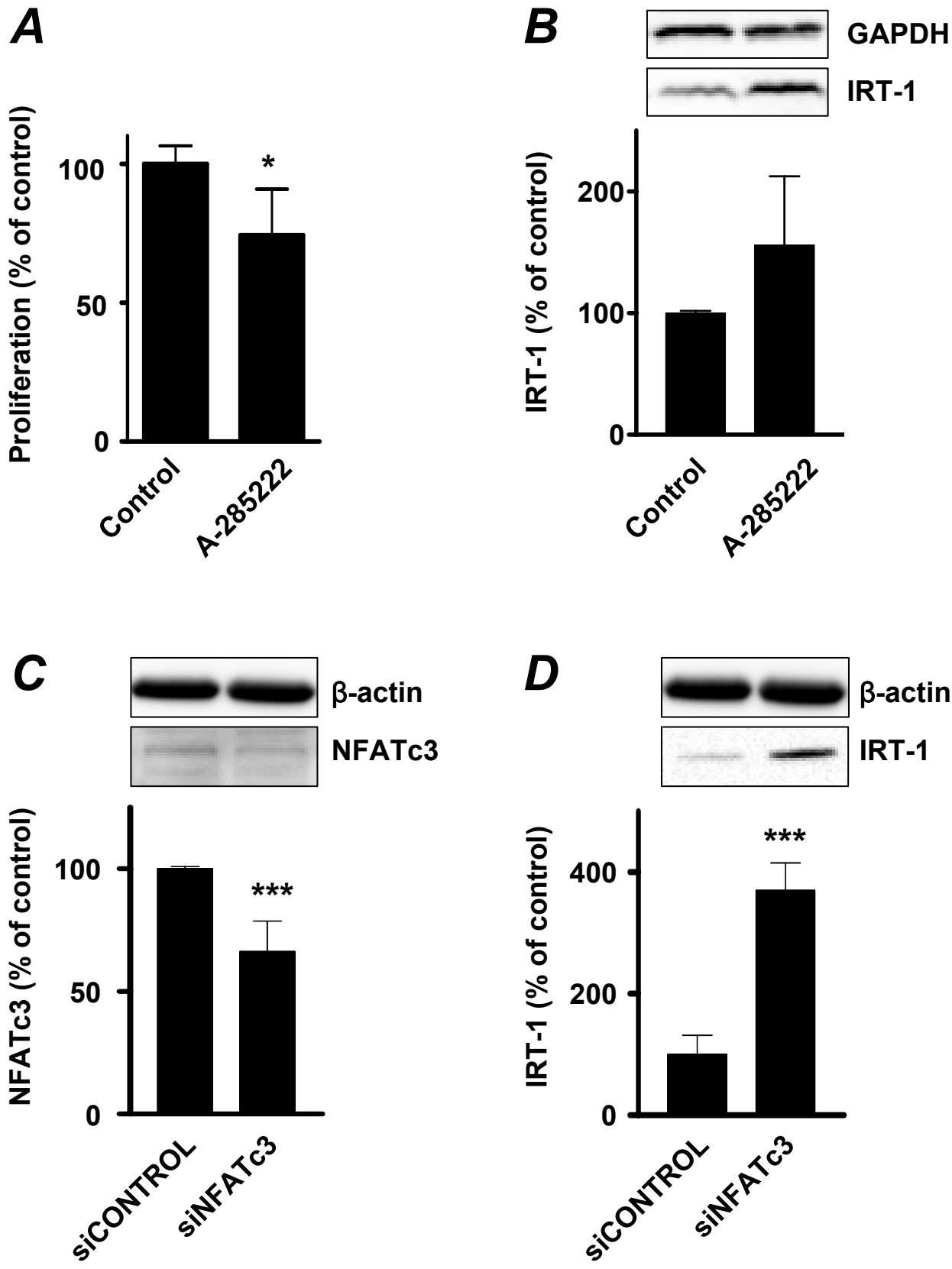
A
Proliferation (% of control)
100
50
0
*
Control
A-285222
B
GAPDH
IRT-1
IRT-1 (% of control)
200
100
0
Control
A-285222
C
β-actin
NFATc3
NFATc3 (% of control)
100
50
0
***
siCONTROL
siNFATc3
D
β-actin
IRT-1
IRT-1 (% of control)
400
200
0
***
siCONTROL
siNFATc3

Fig. 5

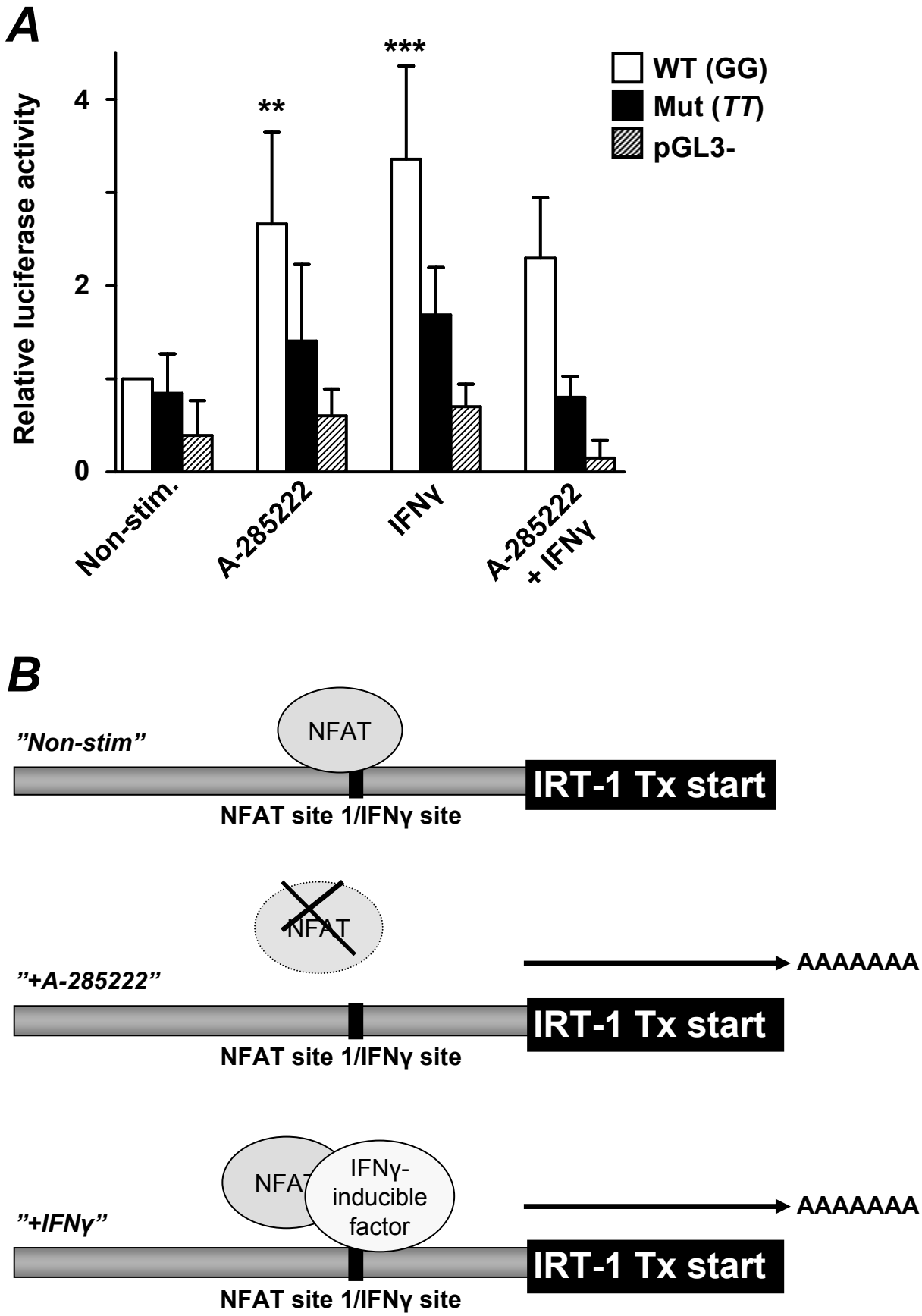
A
Relative luciferase activity
4
2
0
**
***
WT (GG)
Mut (TT)
pGL3-
Non-stim.
A-285222
IFNγ
A-285222 + IFNγ
B
"Non-stim"
NFAT
IRT-1 Tx start
NFAT site 1/IFNγ site
NFAT
AAAAAAA
"+A-285222"
IRT-1 Tx start
NFAT site 1/IFNγ site
NFAT
IFNγ-inducible factor
AAAAAAA
"+IFNγ"
IRT-1 Tx start
NFAT site 1/IFNγ site

Fig. 6

## SUPPLEMENTARY MATERIAL and METHODS

*Human resistance arteries and organ culture.* Intramyometrial resistance arteries from premenopausal women undergoing hysterectomy for non-oncologic reasons were used. Arteries (mean lumen diameter 190 µm, 4-6 cell layers) were dissected in $Ca^{2+}$-free ice-cold physiological saline solution. Vessels were used directly after dissection or after organ culture in DMEM and Ham's F-12 (1:1) supplemented with 50 U/mL penicillin and 50 µg/mL streptomycin. This study conforms to the principles outlined in the Declaration of Helsinki and was conducted in accordance with approved local ethical guidelines (approval reference no. LU 39-02). All women gave their informed consent to participate.

*Cells and cell culture.* Human myometrial vascular smooth muscle cells (VSMCs) were obtained from explants of myometrial arteries as previously described[1] and cultured in DMEM and Ham's F-12 (1:1) with 15% fetal bovine serum (FBS). Human coronary artery smooth muscle cells (HCASMC, Cascade Biologics) were cultured in M231 supplemented with Smooth Muscle Growth Supplement (SMGS). Rat arterial VSMCs were prepared from explants of thoracic aorta as previously described[2, 3] and cultured in DMEM (GIBCO-BRL) with 10% FBS supplemented with 2 mmol/L L-glutamine. 50-100 U/mL penicillin and 50 µg/mL streptomycin were added to the cultures. Cells were used between passages 3 and 8, except for HCASMCs, which were used up to passage 16. The NFAT blocker A-285222[4] was kindly provided by Abbott Laboratories (Abbott Park, IL).

*Human carotid plaque biopsies:* One hundred and fifty eight human carotid plaques collected at carotid endarterectomies and corresponding plasma samples collected the day before surgery were analyzed (Table 1). The indications for surgery were plaques associated with ipsilateral symptoms (transient ischemic attacks-TIA, stroke or amaurosis fugax) and stenosis greater than 70%, or plaques not associated with symptoms but stenosis >80%. Patients with ipsilateral carotid artery occlusion or restenosis after previous carotid endarterectomy were excluded from this study. Cardiovascular risk factors, such as hypertension (systolic blood pressure >140 mm Hg), diabetes, coronary artery disease, smoking (in the past or currently), fasting lipoproteins (total cholesterol, HDL cholesterol, LDL cholesterol and triglycerides) were recorded, as well as the use of medications (anti-hypertensive drugs, diabetes treatment, and statins). All patients were preoperatively assessed by a neurologist. After surgical removal, plaques were snap-frozen in liquid nitrogen at the operating room. Plaques were weighed; cross-sectional fragments of one-mm from the most stenotic region were taken for histology and adjacent fragments for RNA isolation. The remaining of the plaques were homogenized as previously described[5] for protein and cytokine analyses. The study conforms to the principles outlined in the Declaration of Helsinki and was conducted in accordance with approved local ethical guidelines (approval reference no. 472/2005-LUND). All patients gave their informed consent to participate.

*In vitro transcription and translation.* Expression of AIF-1 and IRT-1 proteins was performed by coupled transcription (T3 polymerase) and translation using [$^{35}$S] Methionine in the TNT reticulocyte lysate system according to the manufacturer's

instructions (Promega, Madison, WI). The samples contained 1 μg of the entire cDNA sequence or 1 μg of the deduced open reading frame (ORF). All cDNA samples were cloned into pBlueScript vector (Stratagene, La Jolla, CA). One fifth of the reaction was analyzed on a 16.5% Tris tricinepolyacrylamide gel (Biorad). Gels were fixed and dried, and labeled proteins detected by autoradiography. DIALIGN-TX[6] was used for the protein alignment shown in Fig 1B. The predicted changes in free energy for the secondary structure of the 5' UTRs were calculated using the *mfold* version 3.2 online program.[7]

*Immunofluorescence confocal microscopy.* Human VSMCs cultured on glass coverslips and sections of human myometrial arteries (10 μm) were stained for AIF-1 and IRT-1 according to a previously described protocol.[1] Arteries or cells were fixed in 4% formaldehyde in PBS, permeabilized with 0.2% Triton X-100 in PBS and blocked with 2% bovine serum albumin (BSA) in PBS. Primary antibodies against AIF-1[8] and IRT-1[9] were applied overnight, and Cy5-labeled secondary antibody (Jackson ImmunoResearch Laboratories) were used. Nuclei were stained with the nucleic acid dye SYTOX Green (Molecular Probes). Cells were examined on a Zeiss LSM 5 laser scanning confocal microscope at 40X magnification and arterial sections were examined at 20X magnification.

*Preparation of adenoviral AIF-1HA and IRT-1 gene.* Adenoviral HA-tagged AIF-1 and GFP have been previously described.[10] Recombinant adenovirus containing the IRT-1 gene was prepared using the AdEasy system with the IRT-1 coding region cloned into the

shuttle vector pAdTrack-CMV. The resultant plasmid was linearized with PmeI digestion and co-transformed into E. coli BJ5183 cells with the adenoviral backbone plasmid pAdEasy-1. Recombinants were selected, and recombination was determined by restriction endonuclease analysis. The linearized recombinant plasmid was transfected into 293 cells, and hightiter viral stocks were prepared and purified by CsCl purification.

*In vivo gene transfer and morphometry of injured arteries.* All animal protocols were approved by the local animal care committee (approval No 3374) and conform to the *Guide for the Care and Use of Laboratory Animals* published by the US National Institutes of Health (NIH publication No. 85-23, revised 1996). Left common carotid artery balloon angioplasty was performed under aseptic surgery conditions for rodents (autoclaved instruments and sterile draping) on male Sprague-Dawley rats (320 to 360 g, 15-16 weeks of age, Charles-River Inc.), under sodium pentobarbital anesthesia (65 mg/kg, IP; Steris Laboratories, Phoenix, AZ) as previously described.[10] The depth of anesthesia was assessed by the toe-pinch reflex procedure and absence of muscular tone. Briefly, a 3-4 cm median or left paramedian incision is made on the neck. The sternomastoid and omohyoid muscles are reflected, exposing the underlying bifurcation of the common carotid artery. The left external carotid artery was identified, cleared of adherent tissue, and the segment to be injured transiently isolated from the internal carotid artery by temporary ligatures, allowing the insertion of a 2-F Fogarty arterial embolectomy catheter (Model 12-060-2F; Baxter Healthcare, Santa Ana, CA). The catheter was guided a fixed distance down the common carotid artery to the aortic arch, inflated with a fixed volume of fluid and withdrawn back to the site of insertion. This

procedure is performed a total of three times. After balloon injury, a cannula was introduced into the common carotid artery and the distal injured arterial segment isolated by temporary clips placed midway in the injured segment and at the orifice of the internal carotid artery. The space isolated was filled with either adenoviral GFP, AIF-1, IRT-1 (final titer $1.25x10^9$ pfu /mL) or PBS. Incubation was allowed to proceed for 15 minutes and then the solution was retrieved, the cannula removed, and blood circulation restored.[11, 12] The wound was closed with sterile non-absorbable sutures and swabbed with Povadyne surgical scrub (7.5% Povidone-Iodine; Chaston). No adverse neurological or vascular effects were observed in any animal undergoing this procedure. Buprenorphine (0.02 mg/kg, subcutaneous) was given as analgesic pre- and 12 hours after surgery.

Fourteen days after surgery, rats were exsanguinated via the vena cava under barbiturate anesthesia (120 mg/kg, IP), vessels harvested after fixation and stained with hematoxylin/eosin for morphometry. as previously described.[10] To verify successful adenoviral gene transfer, immunohistochemistry was performed using sections (5 μm) from injured arteries and antibodies against GFP (rabbit polyclonal, 1:100 dilution, Santa Cruz), HA (mouse monoclonal, 1:200 dilution, Santa Cruz) or IRT-1 (column purified rabbit polyclonal, 1:300.[9]) Biotinylated secondary goat anti-rabbit or anti-mouse antibodies were used (Vector Laboratories) at 1:300 or 1:200 dilutions, followed by avidin-biotin peroxidase complex. Staining was visualized with the substrate diaminobenzidine (DAB; Vector Laboratories) producing a reddish-brown color. For nuclear visualization, sections were counterstained with hematoxylin.

*Proliferation and migration assays.* *In vitro* gene transfer into rat VSMCs was performed by incubation with adenoviral GFP, AIF-1 or IRT-1 (final titer $10^8$ pfu/mL) in DMEM containing 0.5% FBS for 2h at 37°C. Under these conditions, >95% of VSMCs are infected.[10] For measurement of proliferation in rat VSMCs, equal numbers of cells were seeded into 6-well plates at a density of 7000 cells/mL; incubated in DMEM containing 10% FBS. Cells were trypsinized and counted on day 4 and 7, using a standard hemocytometer.[2] For human VSMCs, cells were treated as specified in the text and incubated with MTS-solution (CellTiter 96 AQueous One Solution cell proliferation assay, Promega, Madison, WI) for the last 2h, after which absorbance was measured at 490 nm using a Tecan Infinite M200 instrument (Tecan Nordic AB, Mölndal, Sweden). Migration of rat VSMCs was performed in 0.5% FBS (37°C) using standard Boyden Chambers, as previously described.[13] PDGF-AB (40 ng) was used as a chemoattractant and the number of migrated cells were counted 3h later. The number of migrated cells per high power field (HPF) was counted and shown as means from experiments with three independently infected groups performed in triplicate.

*Western blot.* VSMCs and human myometrial arteries were treated as specified in the text and protein was extracted with an SDS sample buffer. An equal amount of protein was loaded onto SDS-PAGE gels and transferred to a nitrocellulose membrane. Membranes were blocked with 5% non-fat powdered milk and incubated with primary antibodies against AIF-1,[8] IRT-1,[9] NFATc3 (sc-8321, Santa Cruz Biotechnology), GAPDH (Chemicon) and β-actin (GenScript Corporation, Piscataway, NJ). HRP-conjugated

secondary antibodies were used and reactive proteins were visualized by using the enhanced chemiluminescence method.

*RNA isolation and RT-PCR.* Total RNA was isolated from human arteries, VSMCs and plaque biopsies using standard techniques. For simultaneous detection of AIF-1 and IRT-1, reverse transcription was performed as previously described[1] and the cDNA was amplified using primers spanning regions common to both AIF-1 and IRT-1 splice variants (5'- TCA TGT CCC TGA AAC GAA TG-3' and 5'-TGG CTT TTC CTT TTC TCT CG-3') or HPRT (5'- TTG CTG ACC TGC TGG ATT AC-3' and 5'-CTG CAT TGT TTT GCC AGT GT-3'). PCR products were separated by agarose gel electrophoresis. For human carotid plaque biopsies, RNA was treated with DNase (Invitrogen) according to the manufacturer's instructions, prior to cDNA synthesis with RevertAid First Strand cDNA Synthesis Kit (Fermentas Life Sciences). AIF-1 and IRT-1 mRNA levels were quantified by real-time RT-PCR using TaqMan Gene Expression Assay Hs00894884_g1 for AIF-1 and Hs9999901_s1 for the housekeeping gene 18S. The IRT-1 assay was custom made and is composed of the following primers and probe: 5'-GTC CCG ACC CCA TCC CTA-3' (forward), 5'- GGA TGT GAG GGT GGA AGG G-3' (reverse) and 5'- FAM-TCC ATA GTC CTG GTC CCC-3' (probe). For human myometrial arteries and VSMCs, expression of AIF-1 and IRT-1 were normalized to the housekeeping genes HPRT and cyclophilin A (Taqman Gene Expression Assays # 4326321E and 4326316E, respectively). All assays were from Applied Biosystems. The PCR reactions were run on an ABI 7900 HT instrument (Applied Biosystems), and the

relative quantity of AIF-1 and IRT-1 mRNA was calculated using the comparative threshold method (delta Ct-method).

*Small interfering RNA (siRNA) transfection.* Human VSMCs were transfected with NFATc3 ON-TARGET plus SMART pool siRNA (Dharmacon) or siCONTROL Non-Targeting siRNA pool (Dharmacon), complexed with Lipofectamine 2000 (Invitrogen) in antibiotics free medium, according to the manufacturer's instructions and as previously described.[1] The cells were incubated with siRNAs at a final concentration of 100 nM for 6h, and further incubated for 5 days in medium containing 1.5% FBS. NFATc3 and IRT-1 expression was determined using Western blot analysis as described above. Transfection efficiency was determined by measuring uptake of a fluorescently labeled siRNA (siGLO Lamin A/C siRNA, 82.5 nM, Dharmacon). Twenty-four hours after transfection start, approximately 90% of the cells were positive for siGLO Lamin A/C siRNA.

*DNA Constructs and Site-directed Mutagenesis.* The genomic DNA fragment of the human AIF-1 gene 5'-flanking region was amplified by PCR and a region spanning from -1529 to +231 relative to AIF-1 translation start site (see Supplemental Fig. 5) was cloned into a pCR2.1-TOPO vector (Invitrogen) according to the manufacturer's instructions. Mutations were introduced with the QuikChange Site-Directed Mutagenesis Kit (Stratagene) using the following primers: 5'- TAA TTT TTT TCA CCC CAC AGG ATT AAA AGC TTT CGG ACT GCT GAA G-3' and 5'- CTT CAG CAG TCC GAA AGC TTT TAA TCC TGT GGG GTG AAA AAA ATT A-3'. The wildtype and mutated AIF-

1 promoter region were excised using KpnI and XhoI restriction enzymes and ligated into a linearized pGL3 Basic Luciferase Vector (Promega) using T4 DNA Ligase (Fermentas Life Sciences), all according to the manufacturer's instructions. The vectors were electroporated into ElectroMAX DH10B *E. Coli* cells (Invitrogen) and plasmid DNA was isolated using GenElute Plasmid Miniprep Kit (Sigma-Aldrich) or plasmid Maxi Kit (Qiagen). All constructs and mutations were verified by sequencing using the Big Dye Terminator v3.1 Cycle sequencing kit (Applied Biosystems) according to the manufacturer's instructions.

*Transfection and luciferase reporter assay:* HCASMC were seeded in 24-well plates at a concentration of 25 000 cells/well and cultured overnight. Transfection was performed by mixing 0.8 μg plasmid DNA (wildtype or mutated AIF-1) or empty pGL3 basic vector (Promega Corporation, WI, USA) with 2 μl Lipofectamine 2000 (Invitrogen) before adding it to the cells. Transfected cells were cultured in M231 supplemented with SMGS for 24h before stimulation with A-285222 (Abbott Laboratories) or interferon γ (IFNγ; Millipore Corporation) as specified in the text. At the end of the stimulation period, transfected cells were lysed in Passive Lysis Buffer (Promega) and luminescence was measured as previously described.[1] Briefly, luciferase substrate reagent (100 mM Tris-HCl pH 7.8, 10 mM MgAcetate, 1 mM EDTA, 1.4 mM luciferin (Promega) and 18.3 mM ATP) was added to the cell lysate and luminescence was measured using a Tecan Infinite M200 instrument (Tecan Nordic AB, Mölndal, Sweden). Luminescence was normalized to protein content as determined by Bradford assay (BioRad) and expressed as relative luminescence units.

*Cytokine assessment.* Cytokine levels were measured in aliquots of 50 μL human carotid plaque homogenates or plasma. Plaque samples were centrifuged at 13.000 g for 10 minutes and 25 μL of the supernatant, or plasma, was used for measuring the following cytokines: eotaxin, fractalkine, IFNγ, interleukin (IL)-10, IL-12(p70), IL-12(p40), IL-1β, IL-6, monocyte chemoattractant protein-1 (MCP-1), macrophage inflammatory protein-1beta (MIP-1β), platelet derived growth factor-AB/BB (PDGF-AB/BB), regulated on activation normal T cell expressed and secreted (RANTES), vascular endothelial growth factor (VEGF), soluble CD40 ligand (sCD40L) and tumour necrosis factor-alpha (TNF-α). Plaque cytokines were normalized to plaque wet weight. The procedure was performed according to the manufacturer's instructions (Milliplex Kit - Human Cytokine/Chemokine Immunoassay - Cat. No.: MPXHCYTO-60K-15 Kit Lots #1691735 and 1702424, Millipore, Electrabox Diagnostica AB, USA) and analyzed with Luminex 100 IS 2.3 (Austin, Texas).

*Plaque immunohistochemistry.* Sections of the one-mm-thick fragment of carotid atherosclerotic plaques were thawed, fixed with ice-cold acetone and permeabilized in 0.5 % Triton-X100 before blocking in 10 % serum. Primary antibodies for CD68 (1:100 dilution, DakoCytomation, Glostrup, Denmark) and α-actin (1:50 dilution, M0851, DakoCytomation, Glostrup, Denmark) were used together with biotinylated secondary rabbit anti-mouse (1:200 dilution, DakoCytomation, Glostrup, Denmark). The DAB detection kit was used for color development (Vector Laboratories). For detection of lipids, sections were fixed with Histochoice (Amresco, Ohio, USA), dipped in 60%

isopropanol and then in 0.4% Oil Red O in 60% isopropanol (for 20 min). Masson's trichrome using Ponceau-acid fuchsin (Chroma-Gesellschaft, Schimdt GmbH, Germany) and aniline blue (BDH, Dorset, England) was used to assess plaque collagen content. To assess the calcified areas, the area of the holes where calcium had been present was measured. Mounted slides were scanned with ScanScope Console Version 8.2 (LRI imaging AB, Vista Californien, USA) and photographed with Aperio image scope v.8.0 (Aperio, Vista, Californien, USA). The area of the plaque (% area) constituted by the different components was quantified blindly using Biopix iQ 2.1.8 (Gothenburg, Sweden).

*Statistics.* For *in vitro* studies, results are expressed as means ± SD, where applicable and statistical analyses were performed using GraphPad software (Prism 4.0). Statistical significance was determined using two-tailed Student's t-test, or one-way analysis of variance followed by Bonferroni test. For analysis of AIF-1 and IRT-1 in human carotid plaques, SPSS version 17.0 was used with Mann-Whitney non-parametric test for determination of statistical difference between two groups, and bivariate correlation analysis to assess non-parametric correlations. Correction for multiple testing was not performed. *$p < 0.05$, **$p < 0.01$ and ***$p < 0.001$.

**References**

1. Nilsson LM, Sun Z-W, Nilsson J, Nordstrom I, Chen Y-W, Molkentin JD *et al.* Novel blocker of NFAT activation inhibits IL-6 production in human myometrial

arteries and reduces vascular smooth muscle cell proliferation. *Am J Physiol Cell Physiol* 2007;**292**:C1167-1178.

2. Autieri MV, Carbone CM. Overexpression of allograft inflammatory factor-1 promotes proliferation of vascular smooth muscle cells by cell cycle deregulation. *Arterioscler Thromb Vasc Biol* 2001;**21**:1421-1426.
3. McMurray HF, Parrott DP, Bowyer DE. A standardised method of culturing aortic explants, suitable for the study of factors affecting the phenotypic modulation, migration and proliferation of aortic smooth muscle cells. *Atherosclerosis* 1991;**86**:227-237.
4. Djuric SW, BaMaung NY, Basha A, Liu H, Luly JR, Madar DJ *et al.* 3,5-bis(trifluoromethyl)pyrazoles: A novel class of NFAT transcription factor regulator. *J Med Chem* 2000;**43**:2975-2981.
5. Goncalves I, Moses J, Dias N, Pedro LM, Fernandes e Fernandes J, Nilsson J *et al.* Changes related to age and cerebrovascular symptoms in the extracellular matrix of human carotid plaques. *Stroke* 2003;**34**:616-622.
6. Subramanian AR, Kaufmann M, Morgenstern B. Dialign-tx: Greedy and progressive approaches for segment-based multiple sequence alignment. *Algorithms Mol Biol* 2008;**3**:6.
7. Zuker M. Mfold web server for nucleic acid folding and hybridization prediction. *Nucleic Acids Res* 2003;**31**:3406-3415.
8. Autieri MV, Carbone C, Mu A. Expression of allograft inflammatory factor-1 is a marker of activated human vascular smooth muscle cells and arterial injury. *Arterioscler Thromb Vasc Biol* 2000;**20**:1737-1744.

9. Autieri MV, Agrawal N. IRT-1, a novel interferon-gamma-responsive transcript encoding a growth-suppressing basic leucine zipper protein. *J Biol Chem* 1998;**273**:14731-14737.

10. Sommerville LJ, Kelemen SE, Autieri MV. Increased smooth muscle cell activation and neointima formation in response to injury in AIF-1 transgenic mice. *Arterioscler Thromb Vasc Biol* 2008;**28**:47-53.

11. Clowes AW, Schwartz SM. Significance of quiescent smooth muscle migration in the injured rat carotid artery. *Circ Res* 1985;**56**:139-145.

12. Tulis DA, Durante W, Liu X, Evans AJ, Peyton KJ, Schafer AI. Adenovirus-mediated heme oxygenase-1 gene delivery inhibits injury-induced vascular neointima formation. *Circulation* 2001;**104**:2710-2715.

13. Autieri MV, Kelemen SE, Wendt KW. AIF-1 is an actin-polymerizing and Rac1-activating protein that promotes vascular smooth muscle cell migration. *Circ Res* 2003;**92**:1107-1114.

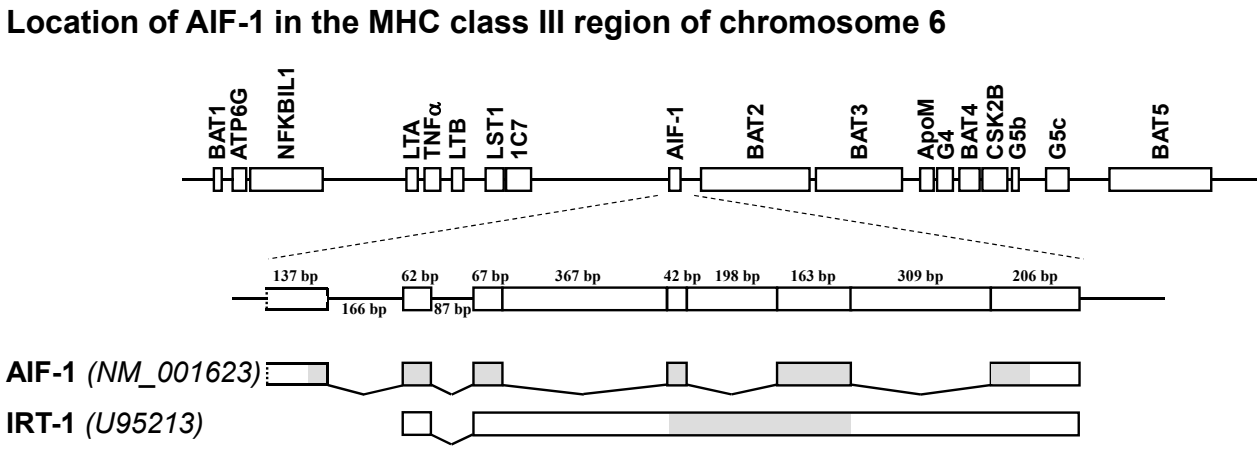


**Figure S1. AIF-1 and IRT-1 are splice variants of the AIF-1 gene.** Schematic representation of part of the human MHC class III region on chromosome 6, harboring the AIF-1 gene. Below is the exon/intron (boxes/lines) organization of the alternative transcripts of AIF-1 and IRT-1 (GenBank accession numbers NM_001623 and U95213, respectively). Exon/intron junctions of these transcripts conform to the consensus GT/AG rule of donor/acceptor splice site recognition. AIF-1 and IRT-1 protein coding sequences of the mRNA are shown in grey and untranslated regions (UTRs) in white.

***Fig. S1***

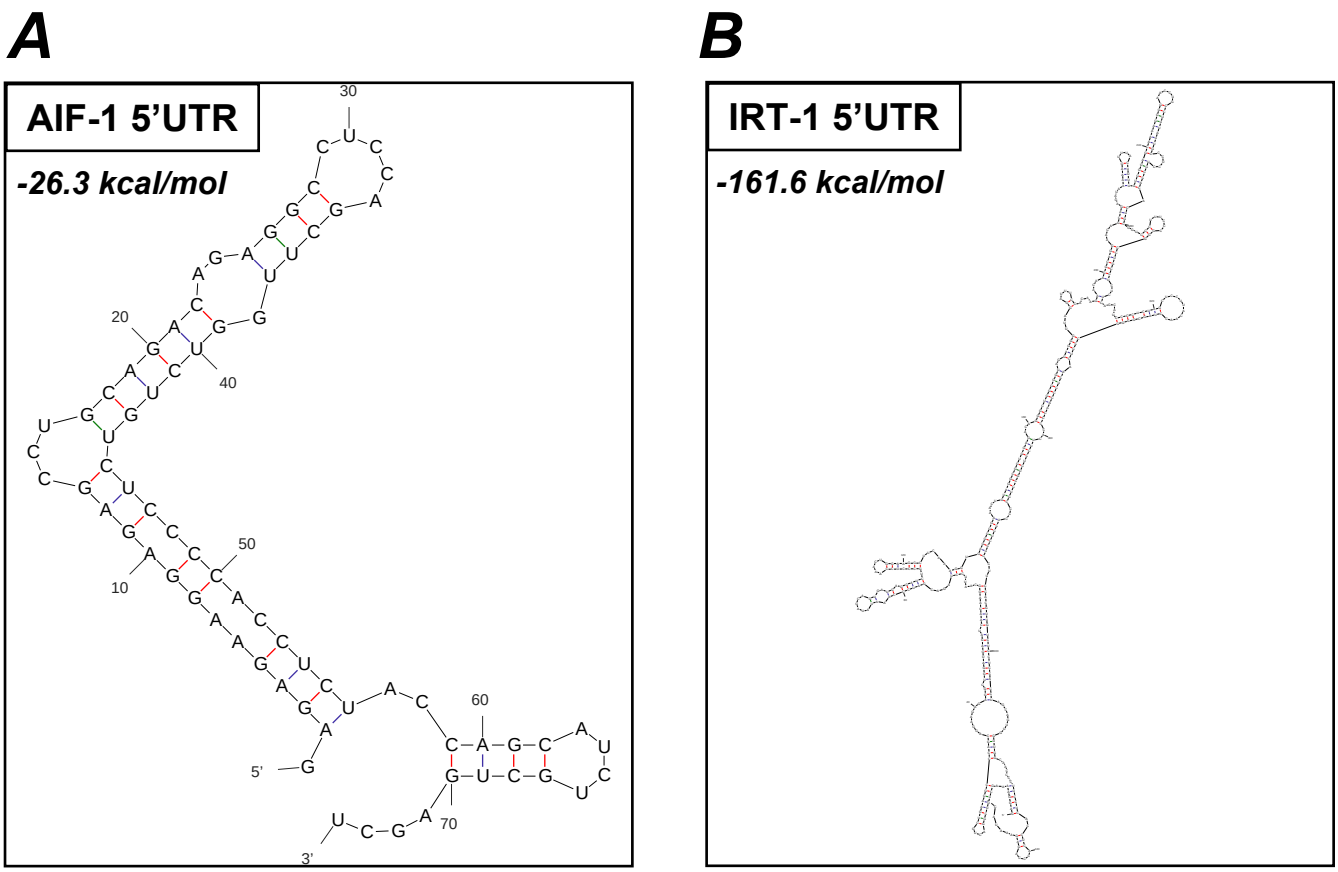


**Figure S2. The secondary structure of the 5' UTRs predicted using the *mfold* version 3.2 online program is shown for AIF-1 (A) and IRT-1 (B)**. The 74 nt 5' UTR of AIF-1 was predicted to yield a change in free energy of -26.3 kcal/mol. For the 453 nt long 5'UTR of IRT-1, the predicted change in free energy was -161.6 kcal/mol.

***Fig. S2***

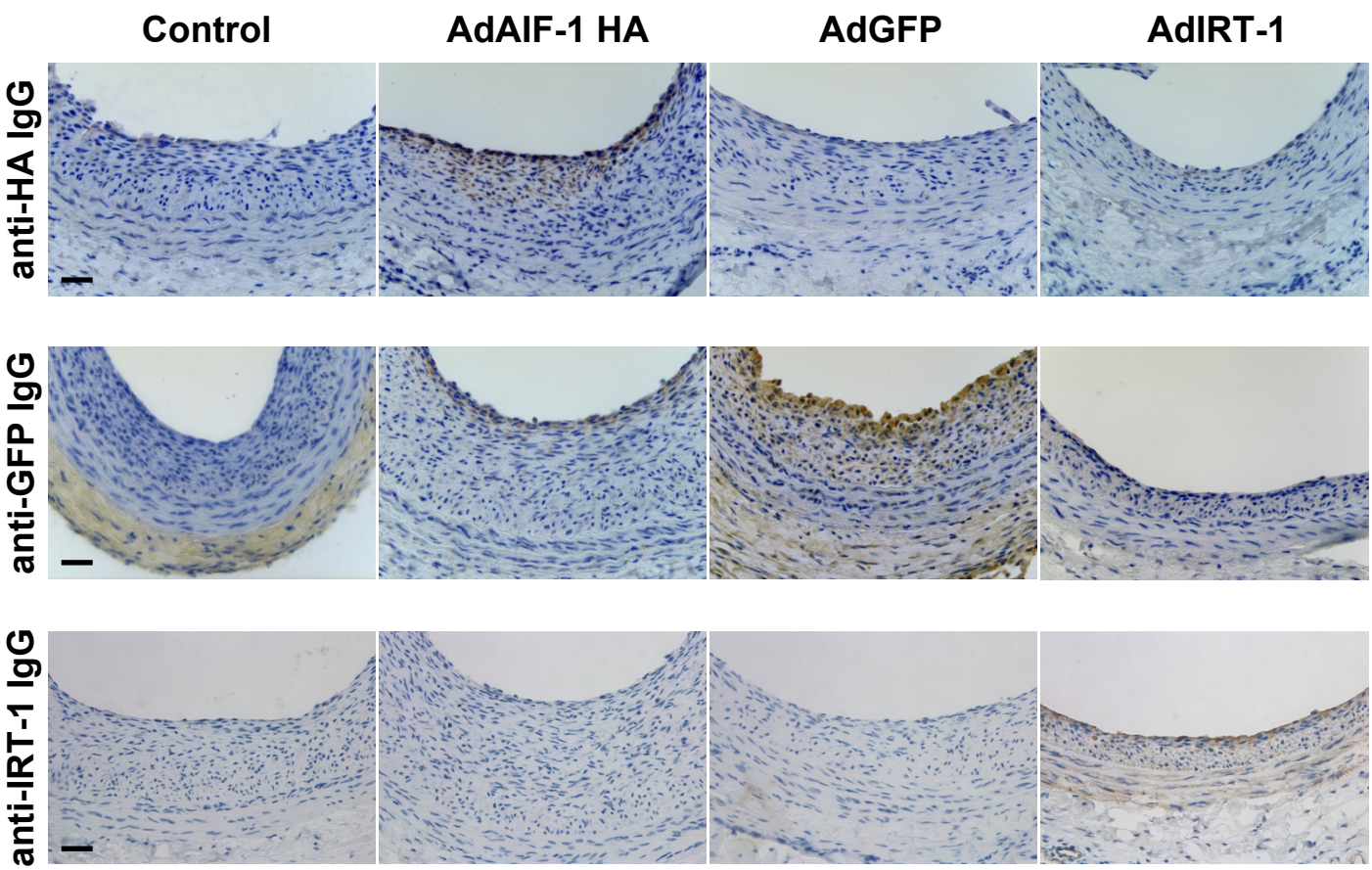


**Figure S3. Adenoviral gene transfer results in protein over expression in the vascular wall.** Representative sections from balloon-injured carotid arteries treated as in Figure 2A are shown. Injured arteries were infected with AdAIF-1, AdIRT-1 and AdGFP, or vehicle (PBS) and after 14 days, vessels were harvested and prepared for immunohistochemistry. Sections were stained with antibodies against either HA (for HA-tagged AIF-1, upper panels), GFP (middle panels) or IRT-1 (lower panels) and red-brown indicates positive immunoreactivity (400x magnification). All sections were counterstained with hematoxylin to visualize the nuclei. Scale bars=50 μm.

***Fig. S3***

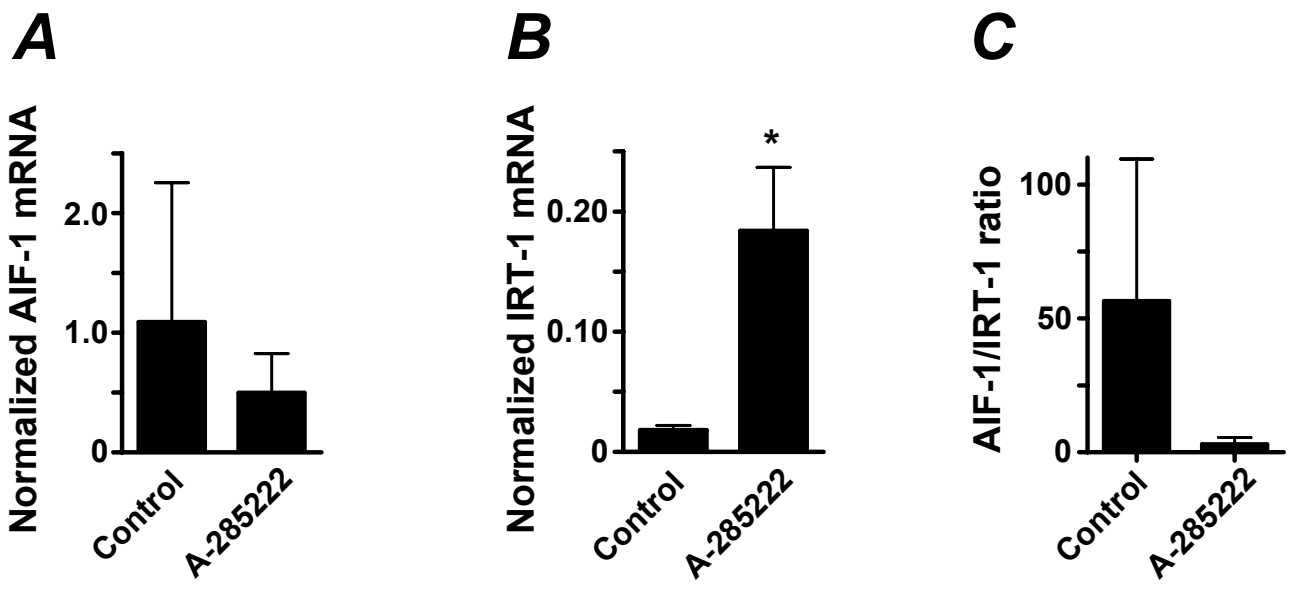


**Figure S4. Inhibition of NFAT with A-285222 increases IRT-1 mRNA expression in VSMCs.** Summarized data from quantitative real-time PCR showing **A.** AIF-1; **B.** IRT-1 mRNA expression and **C.** AIF-1/IRT-1 ratio in HCASMCs. The cells were cultured for 6-9 h in the presence or absence of A-285222 (1.0 μM). Expression of AIF-1 and IRT-1 was normalized to HPRT and cyclophilin A. *$p<0.05$ vs. control, n=3.

*Fig. S4*

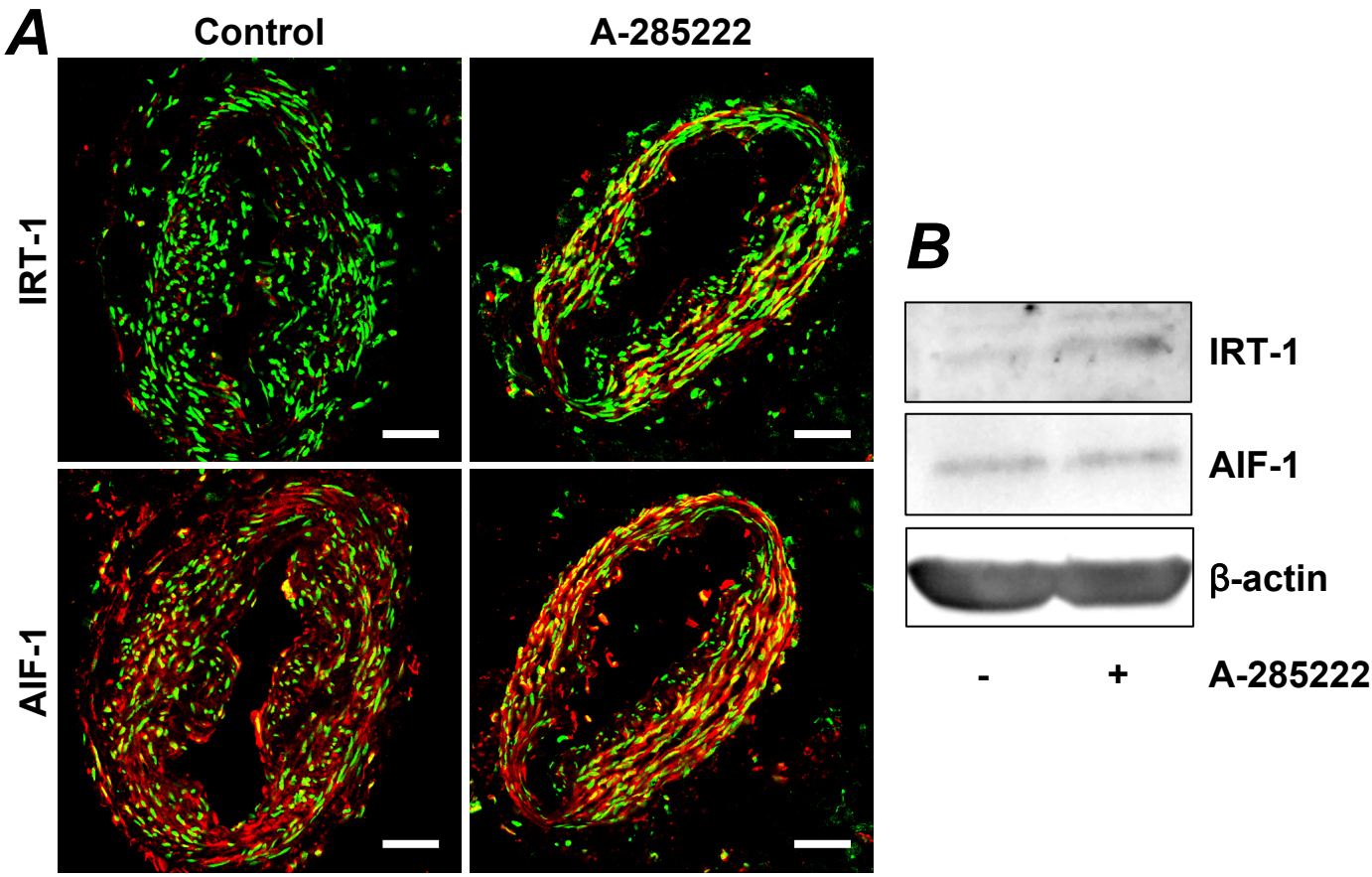


**Figure S5. Inhibition of NFAT increases IRT-1 protein expression in human resistance arteries. A.** Confocal images showing sections from myometrial arteries that had been cultured for 3 days in the presence or absence of the NFAT blocker A-285222 (0.1 μM). Left panels show sections from the same control artery immunostained for either IRT-1 or AIF-1 (both in red); right panels show sections from the same A-285222-treated artery. Nuclei were stained with Sytox Green. Scale bars = 50 μm. Results are representative of 2 experiments including 6 arteries for each condition. **B.** Western blot showing expression of IRT-1 (upper panel) and AIF-1 (middle panel) protein in arteries treated as in A. Expression of β-actin was used to verify equal loading.

***Fig. S5***

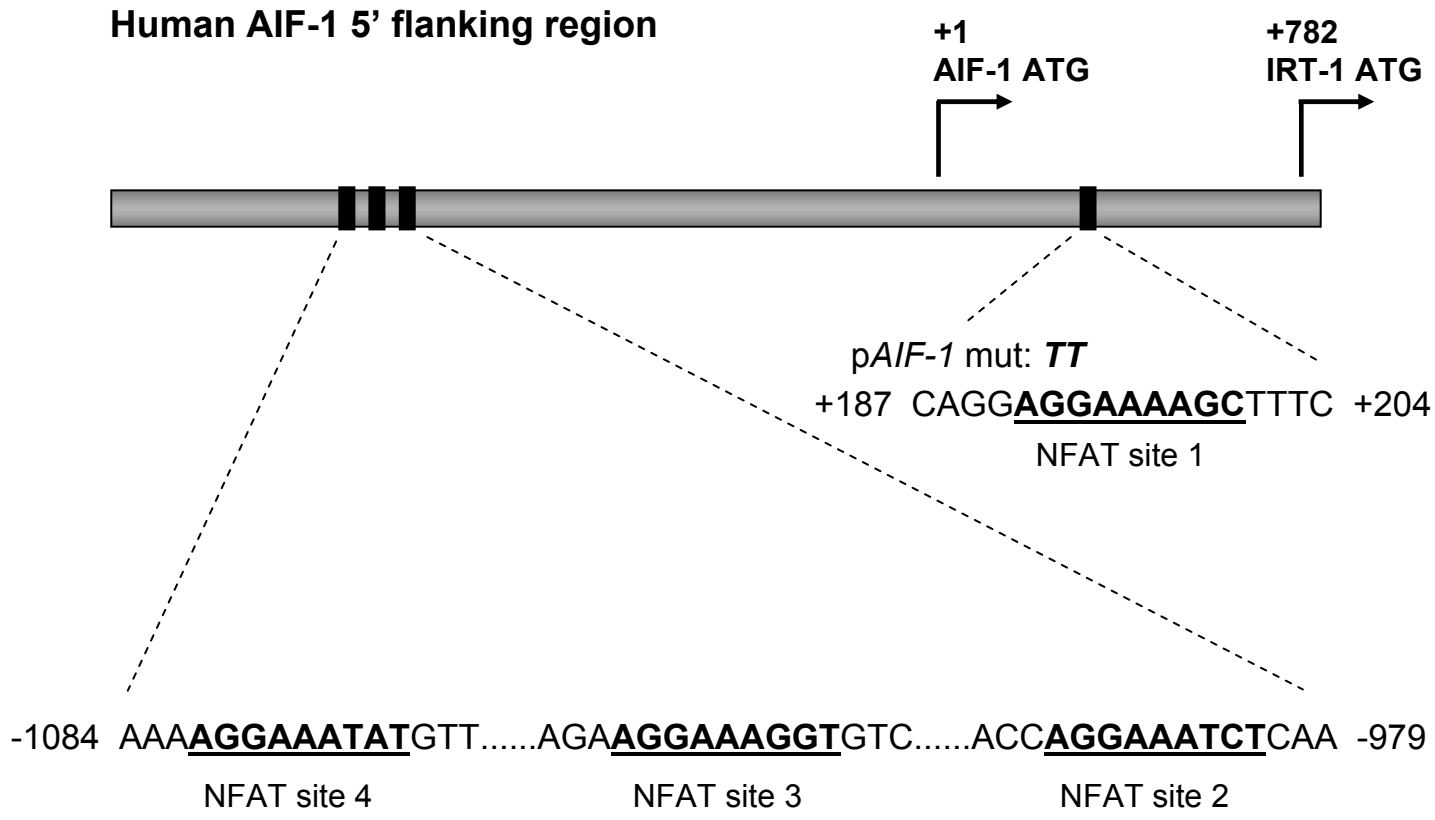


**Figure S6. NFAT binding sites in the human AIF-1/IRT-1 promoter.** Schematic representation of a ~2 kb region of the human genome upstream the IRT-1 protein coding region showing the location and sequences of NFAT binding sites 1-4. Numbers are relative to the AIF-1 translation start site.

***Fig. S6***